5-3-2017

Application of UV Light Scattering to Detect Reversible Self-association and Aggregation of Proteins in Solution

Japneet Kaur
University of Connecticut - Storrs, japneet1989@gmail.com

Application of UV Light Scattering to Detect Reversible Self-association and Aggregation of Proteins in Solution

Japneet Kaur, Ph.D.

University of Connecticut, 2017

ABSTRACT

Monoclonal antibodies and their derivatives have emerged as one of the most successful class of biologics in the past few decades. Antibodies are often formulated at high concentrations in order to achieve the desired therapeutic levels on subcutaneous administration. Reversible self-association and aggregation are two of the major challenges associated with formulating high concentration antibodies. The use of static light scattering as a tool for characterizing self-association and aggregation in protein solutions is reviewed. A detailed understanding of the effect of absorption on Rayleigh light scattering intensity and turbidity was developed for wavelengths where both scattering and absorption occur simultaneously. Macromolecular solutions of tyrosine-starch mixtures, bovine serum albumin and a monoclonal antibody were used to understand the interdependence of Rayleigh scattering (at 90º angle) and light absorption. Results from the studies show that at wavelengths less than 300 nm, 90º scattering intensity decreases as a function of chromophore concentration and depends on molar absorptivity, molecular weight and concentration of molecules. Furthermore, at wavelengths of 300 – 360 nm, Rayleigh scattering intensity for macromolecular solutions was independent of chromophoric absorption. Additionally, turbidity of tyrosine-starch mixtures was also measured in the wavelength range of 250 – 360 nm. Turbidity of starch in the mixtures was independent of the

tyrosine concentration at all wavelengths. These findings suggest that the decrease in 90º scattering intensity observed at 250 – 300 nm for starch-tyrosine mixtures and proteins is because of the reabsorption of scattered light by absorbing chromophores.

A novel method called UV light scattering, was developed to detect reversible and irreversible aggregation by using static light scattering intensities in the UV range. The studies demonstrate that UV light scattering can be used as a fast and rapid tool for detecting reversible and irreversible aggregation in proteins at a wide range of concentrations. It can be used in high-throughput mode for screening different solution conditions and optimizing protein formulations at an early development stage.

Application of UV Light Scattering to Detect Reversible Self-association and Aggregation of Proteins in Solution

Japneet Kaur

B. Pharm., University of Delhi, 2011

A Dissertation

Submitted in Partial Fulfillment of the

Requirements for the Degree of

Doctor of Philosophy

at the

University of Connecticut

2017

APPROVAL PAGE

Doctor of Philosophy Dissertation

Application of UV Light Scattering to Detect Reversible Self-association and Aggregation of Proteins in Solution

Presented by

Japneet Kaur, B. Pharm.

Major Advisor _____
Devendra S. Kalonia

Associate Advisor _____
Michael J. Pikal

Associate Advisor _____
Robin H. Bogner

University of Connecticut
2017

Dedication

To my loving family

Acknowledgements

There are so many people to thank who helped me during the past years and made my stay at UConn a lot easier than I thought it was going to be.

First of all, I express my deepest gratitude to my major advisor, Dr. Devendra S. Kalonia, for giving me the opportunity to work in his lab. I am grateful for his invaluable guidance, patience and immense knowledge. He helped cultivate in me a sense of self-reliance and independent thinking. I am especially thankful for the intense group meetings, his challenging questions and insightful scientific discussions, which helped me build a strong fundamental understanding of my work. I am thankful for his advice, both professional and personal, which has made me a better scientist and an even better person. I feel fortunate to have had the wonderful opportunity to work and learn under his guidance!

I would also like to express my most sincere gratitude to my associate academic advisors, Dr. Michael J. Pikal and Dr. Robin H. Bogner. Dr. Pikal's enthusiasm about science is infectious and inspiring. I hope to acquire as many characteristics as Dr. Pikal possesses as I possibly can, fully aware that it is an impossible task. I am thankful for his constant support and immense faith in my abilities. Dr. Bogner is a meticulous thinker and a very methodical scientist. Her approach to science has helped me think about my work from different directions. They have not only helped me build my fundamental concepts and provided scientific inputs for improving my research, but have also given me important career advice and opportunities when I needed them the most.

I am truly honored to have mentors like you and hope to take your names to greater heights!

I am grateful to the Pharmaceutical Sciences and Pharmaceutics faculty for offering intensive coursework and organizing multidisciplinary seminars which helped me build a strong scientific foundation. A special thanks for the guidance and support provided during the course of my teaching assistantship.

I would also like to thank:

- Past and present administrative staff members at the School of Pharmacy: Leslie LeBel, Mark Armati, Kathy Koji, Liz Anderson, Mina Boone, Jackie Maliga, Sharon Giovenale, Skip Copeland and others for their help and support throughout my graduate studies.
- Department of Pharmaceutical Sciences and Graduate School at University of Connecticut, for providing financial support during my graduate research work.
- Abbott Bioresearch Center and Drs. Michael Seidler and Vineet Kumar for giving me the opportunity to work as a summer intern. It was a great learning experience.
- Don Hoy and Dr. Mu-Ping Nieh for training me and allowing me to use the facilities in their lab.

I would like to express my gratitude to all my past and present labmates: Shermeen, Shubhadra, Nitin, Rajni, Ashlesha, Elisabeth, Masha, Lauren and Liz for being great labmates and helping me both inside and outside the lab. A special thanks to Masha for her constant guidance and friendship throughout my PhD. Thank you for your scientific feedbacks and constant encouragement. Thank you to Lauren for being an amazing labmate, a great friend and a source of guidance to the world outside of school.

Thank you to all my friends at UConn: Leepakshi, Aditya, Mike, Arushi, Vipul, Rajan, Janki, Namita, Shreya, Priya, Ekneet, Upasana, Megha, Sumit, Pavel and others for wonderful memories and unforgettable times.

I also want to thank my friends outside of UConn: Pankaj, Swati, Winnie, Gaurav, Veena, Guncha, Nimisha, Shubhika, Rahul, Navneet and Harpreet for always being just a phone call away. Thank you so much for keeping me in check with the world outside of graduate school and for allowing me to have fun distractions from studies.

A HUGE thank you to Liz Zecca for not only being a great labmate but also being my best friend and a sister I never had! Thank you for all the intense scientific discussions, wonderful memories, inside jokes, funny mischiefs and a never ending support. I could not have survived the ups and downs of graduate school without you, Lizzard! I am extremely fortunate to have found a friend like you. Bud, I will truly miss our times together!

Towards the end, my deepest gratitude goes towards my wonderful family, I could not have reached this point in my life without their love and support. I want to express my gratitude to my wonderful in-laws Mrs. Sharda Singh, Mr. Amarjit Singh and Swaran Veerji for their love, support and blessings. I am indebted to my husband, Inderpreet for his unconditional love and support. I could not have made it without his constant support, encouragement and motivation. I thank him for cheering me up on the sad days and celebrating with me on the happy ones! Among many other things, thanks for always trying to understand my research and telling me every day that you are proud of me. The love and encouragement that I received from my brother, Jasmeet Veerji and sister-in-law, Ginni is deeply acknowledged. I thank my dear Veerji for always being a friend, guide and partner in crime. I fall short of words to thank my kind and loving parents, Mrs. Gurjeet Kaur and Mr. Gurcharan Singh,

for always believing in me and encouraging me to live my dreams. I owe them all of my accomplishments and success, and most importantly I thank them for the person that I am today. I love you all and thank you for always being there for me.

Table of Contents

Chapter 1

Introduction, Aims and Organization of the Dissertation

1. INTRODUCTION

The development of protein pharmaceuticals, especially monoclonal antibodies (MAbs), has grown exponentially in the past few decades.[1-7] The industry is now trending towards the development of high concentration protein therapeutics that can be self-administered via the subcutaneous route, to treat chronic diseases such as arthritis and different types of cancers.[8-11] However, challenges such as high solution viscosity and compromised physical stability are encountered when formulating proteins at high concentrations due to enhanced protein-protein interactions (PPI).[12,13]

Currently, different techniques are used to characterize protein solutions under dilute and semi-dilute conditions. For example, ultraviolet absorption spectroscopy is used to measure protein concentrations;[14,15] light scattering,[16-19] and analytical ultracentrifugation[20-22] are used for determining the nature of PPI; circular dichorism,[23,24] fluorescence,[25,26][25,26] and Fourier transform infra-red spectroscopy are used to study the changes in the secondary structure of proteins. The results of the dilute solution studies are used to predict the behavior of proteins at high concentrations.

Reversible (self-association) and irreversible aggregation are two of the major degradation pathways for proteins in solution. Reversible aggregates pose manufacturing and delivery challenges as this can significantly increase solution viscosity.[10,12,27,28] Additionally, bioavailability and pharmacokinetic properties of proteins can also change due to self-association of proteins.[29] Furthermore, the long term storage of self-associated molecules can result in formation of irreversible aggregates.[12] Irreversible protein aggregates can cause fatal immunogenic reactions, decrease drug potency and/or significantly increase solution viscosity.

Thereby, aggregation (reversible and irreversible) negatively affect manufacturing, delivery and quality of protein formulations, making it a critical concern when developing formulations.[10,30,31]

Static light scattering is rapid, non-invasive, and one of the most commonly used technique to characterize molecular weight, protein-protein interactions and aggregation (reversible and irreversible) of proteins in solution.[32-38] The currently available techniques for characterizing these properties are limited to dilute samples. The properties of proteins, however, can be significantly different at high concentrations compared to the predictions made using results of dilute solution studies.[12,24,39] Thus, there is a lack of methods to directly study physical stability of high concentration protein formulations. Furthermore, the current techniques such as AUC are seldom used in early product development because of long experiment times, inability to perform high-throughput analysis, higher level of operator expertize and complex data analysis. This necessitates the development of a technique to characterize the properties of proteins such as self-association and aggregation in a wide range of concentrations and at an early stage in product development. Additionally, such a technique can be used to screen proteins under different solution pH and ionic strengths to optimize the formulation in initial development stages.

2. PROJECT OBJECTIVE

The present work focuses on broadening the application of static light scattering in the ultraviolet wavelength range of 260 – 360 nm. The sensitivity of UV light scattering is investigated to characterize physical instability in proteins in a wide range of concentrations.

This will help in early screening and optimization of high concentration protein and antibody formulations.

3. SPECIFIC OBJECTIVES

The specific aims of this work are:

a. Systematically investigate the effect of absorption on Rayleigh light scattering and turbidity of macromolecular solutions.

b. Characterize reversible self-association of proteins in solution by using ultraviolet static light scattering.

c. Detect and analyze the change in aggregate content of proteins in a wide range of concentrations by ultraviolet static light scattering.

4. CHAPTER ORGANIZATION AND OUTLINE

Chapter 2 reviews the application of static light scattering to characterize different properties of proteins in solutions such as molecular weight, protein-protein interactions, reversible and irreversible aggregation. The basic modern instrumentation for light scattering is discussed along with mathematical concepts that are involved in data analysis. The limitations associated with current static light scattering techniques and aspects of broadening its application to analysis of high concentration protein solutions has been summarized. Some of the key studies in the area of protein-protein interactions, association and aggregation are discussed with a focus high concentration solutions.

Static light scattering intensity increases with the decrease in wavelength of incident light. Thereby, using shorter wavelengths in the ultraviolet range can increase the sensitivity of the technique. Presently available static light scattering instruments for protein analysis use laser light sources with wavelengths greater than 600 nm to avoid interference from other optical phenomenon such as absorption by protein chromophores. **Chapter 3** presents a systematic investigation of the effect of absorption on 90º Rayleigh scattering intensity and turbidity of macromolecular solutions. Solutions of small aromatic amino acid and large macromolecule were used to determine the effect of absorption by amino acids on scattering by macromolecules. The study further extends to understand the effect of molecular weight, molar absorptivity and concentration of proteins on light scattering intensities in ultraviolet range.

After developing an understanding of effect of absorption on static light scattering in the ultraviolet range, the following chapters test the sensitivity of the technique to study physical stability of proteins in solution. **Chapter 4** presents a systematic approach to develop ultraviolet light scattering as a technique to detect reversible self-association of proteins in solution. The studies have been conducted using β-lactoglobulin A and glutamate dehydrogenase as the model proteins. β-lactoglobulin A was chosen for this purpose because its dimerization and association constant under different solution conditions is well characterized. Glutamate dehydrogenase was chosen because it undergoes concentration based reversible self-association, which is a known concern for high concentration monoclonal antibody formulations. This work was critical to investigate the application of ultraviolet light scattering as a high-throughput technique to detect reversible self-association in protein formulations.

The work presented in **Chapter 5** is focuses on investigating the application of ultraviolet static light scattering as a technique to detect changes in aggregates in protein formulations. The

present techniques for measuring aggregates requires dilution of sample to low concentration and the information about concentrated protein behavior goes undetected. Thereby, another purpose of the work was to investigate aggregation in a wide range of protein concentrations. The studies were conducted using bovine serum albumin, β-lactoglobulin and a monoclonal antibody in the concentration range of 2 – 50 mg/mL. The work was useful in expanding the application of static light scattering to the ultraviolet range and investigating its use for detecting aggregation in protein solutions.

Chapter 6 gives a summary of the present research work.

5. REFERENCES

1. Aggarwal, S. What's fueling the biotech engine? *Nat. Biotechnol.* **2007**, *25*, 1097-1104.
2. Aggarwal, S. What's fueling the biotech engine - 2007. *Nat. Biotechnol.* **2008**, *26*, 1227-1233.
3. Aggarwal, S. What's fueling the biotech engine-2009-2010. *Nat. Biotechnol.* **2010**, *28*, 1165-1171.
4. Aggarwal, S. What's fueling the biotech engine-2010 to 2011. *Nat. Biotechnol.* **2011**, *29*, 1083-1089.
5. Aggarwal, S. What's fueling the biotech engine-2011 to 2012. *Nat. Biotechnol.* **2012**, *30*, 1191-1197.
6. Aggarwal, S. R. What's fueling the biotech engine-2012 to 2013. *Nat. Biotechnol.* **2014**, *32*, 32-39.
7. Carlson, R. Estimating the biotech sector's contribution to the US economy. *Nat Biotech* **2016**, *34*, 247-255.
8. Leader, B.; Baca, Q. J.; Golan, D. E. Protein therapeutics: A summary and pharmacological classification. *Nat. Rev. Drug Discov.* **2008**, *7*, 21-39.
9. An, Z. Monoclonal antibodies - a proven and rapidly expanding therapeutic modality for human diseases. *Protein Cell* **2010**, *1*, 319-330.
10. Shire, S. J.; Shahrokh, Z.; Liu, J. Challenges in the development of high protein concentration formulations. *J. Pharm. Sci.* **2004**, *93*, 1390-1402.
11. Goswami, S.; Wang, W.; Arakawa, T.; Ohtake, S. Developments and Challenges for mAb-Based Therapeutics. **2013**, *2*, 452-500.
12. Saluja, A.; Kalonia, D. S. Nature and consequences of protein-protein interactions in high protein concentration solutions. *Int. J. Pharm.* **2008**, *358*, 1-15.
13. Zhou, H. -.; Rivas, G.; Minton, A. P. Macromolecular crowding and confinement: Biochemical, biophysical, and potential physiological consequences. *Annual Review of Biophysics* **2008**, *37*, 375-397.
14. Mach, H. Ultraviolet absorption spectroscopy. *Methods Mol. Biol.* **1995**, *40*, 91; 91-114; 114.
15. Pace, C. N.; Vajdos, F.; Fee, L.; Grimsley, G.; Gray, T. How to measure and predict the molar absorption coefficient of a protein. *Protein Science* **1995**, *4*, 2411-2423.
16. Yadav, S.; Scherer, T. M.; Shire, S. J.; Kalonia, D. S. Use of dynamic light scattering to determine second virial coefficient in a semidilute concentration regime. *Anal. Biochem.* **2011**, *411*, 292-296.
17. Yadav, S.; Shire, S. J.; Kalonia, D. S. Viscosity analysis of high concentration bovine serum albumin aqueous solutions. *Pharm. Res.* **2011**, *28*, 1973-1983.
18. Yadav, S.; Liu, J.; Shire, S. J.; Kalonia, D. S. Specific interactions in high concentration antibody solutions resulting in high viscosity. *J. Pharm. Sci.* **2010**, *99*, 1152-1168.

19. Neal, B. L.; Asthagiri, D.; Velev, O. D.; Lenhoff, A. M.; Kaler, E. W. Why is the osmotic second virial coefficient related to protein crystallization? *J. Cryst. Growth* **1999**, *196*, 377-387.
20. Winzor, D. J.; Deszczynski, M.; Harding, S. E.; Wills, P. R. Nonequivalence of second virial coefficients from sedimentation equilibrium and static light scattering studies of protein solutions. *Biophys. Chem.* **2007**, *128*, 46-55.
21. Ross, P. D.; Minton, A. P. Analysis of non ideal behavior in concentrated hemoglobin solutions. *J. Mol. Biol.* **1977**, *112*, 437-452.
22. Howlett, G. J.; Minton, A. P.; Rivas, G. Analytical ultracentrifugation for the study of protein association and assembly. *Curr. Opin. Chem. Biol.* **2006**, *10*, 430-436.
23. Chari, R.; Singh, S. N.; Yadav, S.; Brems, D. N.; Kalonia, D. S. Determination of the dipole moments of RNAse SA wild type and a basic mutant. *Proteins Struct. Funct. Bioinformatics* **2012**, *80*, 1041-1052.
24. Chari, R.; Jerath, K.; Badkar, A. V.; Kalonia, D. S. Long- and short-range electrostatic interactions affect the rheology of highly concentrated antibody solutions. *Pharm. Res.* **2009**, *26*, 2607-2618.
25. Kumar, V.; Sharma, V. K.; Kalonia, D. S. Second derivative tryptophan fluorescence spectroscopy as a tool to characterize partially unfolded intermediates of proteins. *Int. J. Pharm.* **2005**, *294*, 193-199.
26. Abbas, S. A.; Gaspar, G.; Sharma, V. K.; Patapoff, T. W.; Kalonia, D. S. Application of second-derivative fluorescence spectroscopy to monitor subtle changes in a monoclonal antibody structure. *J. Pharm. Sci.* **2013**, *102*, 52-61.
27. Liu, J.; Nguyen, M. D. H.; Andya, J. D.; Shire, S. J. Reversible self-association increases the viscosity of a concentrated monoclonal antibody in aqueous solution. *J. Pharm. Sci.* **2005**, *94*, 1928-1940.
28. Kanai, S.; Liu, J.; Patapoff, T. W.; Shire, S. J. Reversible self-association of a concentrated monoclonal antibody solution mediated by fab-fab interaction that impacts solution viscosity. *J. Pharm. Sci.* **2008**, *97*, 4219-4227.
29. Brems, D. N.; Alter, L. A.; Beckage, M. J.; Chance, R. E.; Dimarchi, R. D.; Green, L. K.; Long, H. B.; Pekar, A. H.; Shields, J. E.; Frank, B. H. Altering the association properties of insulin by amino acid replacement. *Protein Eng. Des. Sel.* **1992**, *5*, 527-533.
30. Roberts, C. J. Protein aggregation and its impact on product quality. *Curr. Opin. Biotechnol.* **2014**, *30*, 211-217.
31. Jiskoot, W.; Randolph, T. W.; Volkin, D. B.; Middaugh, C. R.; Schöneich, C.; Winter, G.; Friess, W.; Crommelin, D. J. A.; Carpenter, J. F. Protein instability and immunogenicity: Roadblocks to clinical application of injectable protein delivery systems for sustained release. *J. Pharm. Sci.* **2012**, *101*, 946-954.

32. Knobloch, J. E.; Shaklee, P. N. Absolute Molecular Weight Distribution of Low-Molecular-Weight Heparins by Size-Exclusion Chromatography with Multiangle Laser Light Scattering Detection. *Analytical Biochemistry* **1997**, *245*, 231-241.
33. Nguyen, L. T.; Wiencek, J. M.; Kirsch, L. E. Characterization Methods for the Physical Stability of Biopharmaceuticals. *PDA J. Pharm. Sci. Technol.* **2003**, *57*, 429-445.
34. Oliva, A.; Llabrés, M.; Fariña, J. B. Applications of multi-angle laser light-scattering detection in the analysis of peptides and proteins. *Curr Drug Discov Technol* **2004**, *1*, 229-242.
35. Philo, J. S. Is any measurement method optimal for all aggregate sizes and types? *The AAPS Journal* **2006**, *8*, E564-E571.
36. Wyatt, P. J. Multiangle light scattering combined with HPLC. *LC GC: Liquid Chromatography, Gas Chromatography* **1997**, *15*, 160-168.
37. Wyatt, P. J. Multiangle light scattering: The basic tool for macromolecular characterization. *Instrum Sci Technol* **1997**, *25*, 1-18.
38. Wyatt, P. J. Light scattering and the absolute characterization of macromolecules. *Analytica Chimica Acta* **1993**, *272*, 1-40.
39. Scherer, T. M.; Liu, J.; Shire, S. J.; Minton, A. P. Intermolecular interactions of IgG1 monoclonal antibodies at high concentrations characterized by light scattering. *J Phys Chem B* **2010**, *114*, 12948-12957.

Chapter 2

Static Light Scattering as a Tool for Characterizing Reversible Self-association and Aggregation in Protein Solutions

CONTENTS

Chapter 2

1. INTRODUCTION

In the past few decades, monoclonal antibodies (MAbs) and MAb derivatives have emerged as the most successful class of biotherapeutics, for the treatment of chronic diseases such as autoimmune disorders, inflammation and various types of cancers.[1-7] In order to facilitate patient compliance and outpatient administration, pharmaceutical research efforts are being focused on development of formulations for subcutaneous delivery. High concentration formulations are needed for achieving therapeutic level of MAbs via subcutaneous route. Reversible self-association (RSA) and aggregation are two of the major challenges associated with formulating high concentration MAb solutions.[8-10] Static light scattering is one of the most important tools for characterizing different properties of proteins in solution such as molecular weight, protein-protein interactions, and protein self-association.[11-16]

When light hits a molecule, the electromagnetic radiation induces polarity by interacting with the electrons in the molecule. The wave nature of the radiation causes fluctuations in the induced polarity and the electrons of the molecule re-emit radiation of the same frequency in all the directions. This phenomenon of elastic scattering is called static light scattering. The average scattering intensity (i_s) is measured at a fixed angle/angles and i_s depends on the molecular weight and intermolecular interactions of the protein molecules. It is a non-invasive technique in which sample can be recovered for further analysis.

2. INSTRUMENTATION

A variety of SLS instruments are commercially available, with different costs and applicability. The hardware and software used for SLS is discussed in detail in specialized reports,[17-19] however, a brief overview of the instrumentation is provided in this section. All SLS

instruments consist of the following basic components (figure 1): light source, sample holder and detector at fixed angle/angles.

2.1. Light Source

The commercially available SLS instruments use monochromatic laser (such as helium-neon or argon ion) light sources therefore, also referred to as laser light scattering. The laser wavelength (λ_0) can range anywhere between 600 – 700 nm. Higher wavelengths of incident light are used for characterization of biomolecules (such as monoclonal antibodies or mAbs) to prevent interference from other optical phenomena such as absorption and fluorescence.

2.2. Measurement Angle

The SLS measurements are classified based on the angle of measurement as low angle light scattering (LALS, angle close to 0º), right angle light scattering (RALS, 90º), backscattering (angles greater than 90º), and multi-angle light scattering (MALS, simultaneous measurements at different angles). The presence of single or multiple angle/s (θ) of scattering intensity measurement depends on the application of the technique. For example, for molecules of size less than $\lambda_0/20$ the scattering intensity does not have an angular dependence and a single angle measurement is used to characterize size (molecular weight) of the particles. Whereas, for molecules with size comparable to the wavelength of incident light, scattering intensity depends on the angle at which it is measured and instruments with multi-angle measurement capabilities are used to provide information about the shape and size (radius of gyration and molecular weight) of the particles.

2.3. Detector

The detectors can be either a photo diode (cheap but relatively less sensitive) or photomultiplier tube, PMT (expensive but very sensitive). Modern light scattering instruments

are equipped with PMT type of detectors. Some instruments also used flow cells and chromatographic separation techniques before performing SLS measurements and operate in high throughput manner, while others operate in batch mode.

3. APPLICATIONS

The propensity of proteins to self-associate and aggregate is governed by the net effect of various attractive and repulsive intermolecular interactions. Therefore, early detection and characterization of these instabilities is critical for protein formulators. Light scattering intensity is sensitive to these nonspecific interactions and can give information about the intermolecular interactions and weight-average molecular weight of protein species (discussed in the following sections). The results are often used to predict the aggregation propensity of the formulation at high concentration.[20,21]

3.1. Measuring nonideality and weight-average molecular weight

For non-interacting (ideal) scattering species, the time-average scattering intensity (i_s) is related to the molecular weight (M_w) of the scatterer by constructing a Debye plot using the following equation:[17,22,23]

$$\frac{Kc}{R_\theta} = \frac{1}{M_w} \qquad \text{Equation 1}$$

where K is the optical constant, R_θ is the excess Rayleigh scattering ratio, θ is the scattering angle, c and M_w are concentration and weight-average molecular weight of the scattering molecule, respectively and:

$$R_\theta = \frac{i_s}{I_0}\frac{r^2}{(1+cos^2\theta)}$$ Equation 2

where i_s is the scattering intensity, I_0 is the intensity of incident light, r is the distance between the scattering molecule and the detector. The excess Rayleigh ratio depends on instrument constants such as r and θ and these parameters are commonly calibrated using toluene as a standard.

$$K = \frac{4\pi^2 n^2}{N_A \lambda_0^4}\left(\frac{dn}{dc}\right)^2$$ Equation 3

The optical constant K depends on the solution refractive index (n), Avogadro's number (N_A), wavelength of incident light in vacuum (λ_0) and refractive index gradient for the solvent/scattering molecule pair (dn/dc).

For dilute solutions of interacting species such as proteins, the scattering intensity per unit volume is related to molecular weight (M_w) and nonideality parameter (B_2) given by the following equation:[17,23]

$$\frac{Kc}{R_\theta} = \frac{1}{M_w} + 2B_2c + \cdots$$ Equation 4

Under dilute solution limit the Rayleigh ratio (Kc/R_θ) for proteins varies linearly with concentration as shown by equation 4. The weight-average molecular weight and B_2 for proteins are obtained from the intercept and slope, respectively.

Proteins are charged molecules with a surface containing different amino acid residues. These different groups give rise to intermolecular protein-protein interactions (PPIs). B_2 is the thermodynamic second virial coefficient and is used to characterize net PPIs in the solution. A

positive value of B_2 indicates repulsive interactions dominate and a negative value means attractive interactions dominate. When the attractive interactions equal the intermolecular repulsion the value of B_2 is zero. The net PPIs (thereby B_2) depends on the solution conditions such as pH,[21,24-26] ionic strength,[21,24-28] and presence of co-solutes.[29] The B_2 value for Lysozyme becomes more negative on a pH increment of 3.5 to 7.5, indicating an increase in net intermolecular attractions.[26] Furthermore, an increase in sodium chloride (NaCl) concentration also increased the net attractions by shielding the protein charge at pH of 4.5. In a different study by Abbas et al.[29] the effect of addition of polyols on the nature of PPIs in MAbs was studied using B_2 obtained from SLS analysis. The study showed that the value of B_2 became less negative on addition of trehalose or ethylene glycol indicating a decrease in net attractions. Furthermore, the decrease in attractive interactions correlated with the decrease in aggregation for the mAbs in the presence of polyols.

The other important application of SLS is to determine the weight-average molecular weight of the scattering species. Scattering intensity (i_s) is directly proportional to the molecular weight of the scattering species thereby, has been extensively used to determine the molecular weight of polymers, monoclonal antibodies and other proteins. For ideal non-interacting species the molecular weight can be estimated at the *limit of dilution*, by rearranging equation 1 to obtain the following equation:[17,23,30]

$$\frac{R_\theta}{K_0} = \left(\frac{n}{n_0}\right)^2 M_w c_{tot} \qquad \text{Equation 5}$$

where c_{tot} is the total concentration of all the protein species in the solution, n_0 and n is the refractive index of solvent (buffer) and solution, respectively.

According to the concentration fluctuation theory, at *arbitrary protein concentrations*, the molecular weight of proteins can be estimated using the following equation:[30]

$$\frac{R_\theta}{K_0} = \left(\frac{n}{n_0}\right)^2 \frac{M_w}{1 + c\frac{\partial \ln \gamma}{\partial c}} \qquad \text{Equation 6}$$

where γ is the thermodynamic activity coefficient.

3.2. Characterization of Reversible Self-Association in Protein Solutions

Characterization of reversible self-association (RSA) of proteins essentially involves the determination of the association constant, K_a. There is a tremendous interest in studying protein self-association at high protein concentration, however, the difficulty lies in the fact that most of the currently available techniques are limited to dilute concentrations (0 – 10 mg/mL). Among the variety of analytical techniques used to detect and characterize self-association the ones using static light scattering analysis are discussed in the following paragraphs.

Fernández and Minton[31] have used SLS to characterize self-association in chymotrypsin A at three pH values. The scattering data showed the presence of monomer, dimer and depending on the solution pH, either pentamer (pH 4.1 and 5.4) or hexamer (pH 5.4 and 7.2).

In the work by Esfandiary et al.,[32] composition-gradient multiangle static light scattering (CG-MALS) was used as a method for detecting and characterizing RSA in IgG type proteins. The increasing trends in molecular weight indicated the presence of self-association which was calculated using equation 4. This technique however, is limited to a low-throughput format to characterize RSA at later stage rather than a screening tool in early formulation development.

In a different study by Bajaj et al.,[33] protein self-association was characterized by size-exclusion chromatography (SEC) using a flow cell capable of simultaneously measuring protein

concentration and scattered light intensity in a high-throughput format. The Debye scattering equation 4 was modified to include the self-association equilibrium model including equilibrium constant and total protein. The modified equation yielded the value for K_a for the model protein under various solution conditions. The major drawback of SEC is that the samples get diluted and the information about concentration based RSA goes undetected.

3.3. Characterization of Protein Aggregation

The protein aggregates (reversible or irreversible) are larger in size compared to the non-aggregated native form of proteins. The size of the protein aggregates is analyzed by constructing the plot using the following standard form of the Zimm equation[18,22]:

$$\frac{Kc}{R_\theta} = \left(\frac{1}{M_w} + 2B_2c\right)\left[1 + \frac{16\pi^2 R_g^2 sin^2\left(\theta/2\right)}{3\lambda_0^2}\right] \quad \text{Equation 7}$$

where R_g is the square root of the mean square radius of gyration of the scattering particles obtained by analyzing the samples at multiple angles (θ).

In addition to the batch-mode light scattering, size exclusion chromatography with an inline multi-angle light scattering (SEC-MALS) detector has been used to characterize and monitor formation of protein aggregates in solution.[12,34-36] SEC-MALS is based on the separation of species of different molecular weights using the SEC column and then measure scattering intensities at multiple angles. Li et al.[34] characterized the size and polydispersity of high molecular weight soluble aggregates in bovine α-chymotrypsinogen A. The weight-average molecular weight (M_w) and radius of gyration (R_g) of the protein species were obtained using the Zimm equation (equation 8). Figure 2 (taken from Li et al.[34]) shows that the scattering intensity contribution (solid line) by the monomers is less than the HMW aggregates although, the

concentration of monomers is twice that of HMW species. The M_w/M_{mon} ratio for monomers was essentially flat indicating presence of monodisperse monomer species. However, the molecular weight for HMW species ranged from 1000 kDa (~40 M_{mon}) to up to 3000 kDa (~100 M_{mon}). The primary advantage of SEC-MALS compared to conventional SEC is that the former gives absolute M_w without the need for calibration (using M_w standards).

3.4. Use of light scattering at lower wavelengths (UV range)

Scattering intensity is inversely proportional to the fourth power of wavelength (as given by the Rayleigh scattering equation) and increases at lower wavelengths. The commercially used scattering instruments have light sources ranging from 600 – 700 nm to avoid interference from other optical phenomenon such as light absorption or fluorescence. Scattering intensity of Rayleigh scatters with size less than λ/20 is independent of scattering angle. Therefore, the currently available scattering instruments can be used to measure sizes of particles greater than 60 – 70 nm. Protein aggregates however, can range from 10 to a few hundred nm.

In the work by Chen et al.,[37] the authors used UV light scattering spectroscopy to detect nanoscale particles. They used the backscattered light in the UV range (250 to 390 nm) to determine the sizes of nanoparticles. The mean size of the particles was 33, 41, 63 and 84 nm. The study suggests that the high sensitivity and accuracy of UV light scattering may find potential applications for studying and detecting macromolecular complexes. This technique can therefore, be useful for providing information of protein self-association and aggregation in solutions.

4. RELATIONSHIP BETWEEN STATIC LIGHT SCATTERING AND TURBIDITY

Light scattering intensities have been measured in the UV range in terms of turbidity which is defined as the total light scattered in all the directions. It is often measured as the light attenuated by non-absorbing species using a UV spectrometer. The mathematical relationship between turbidity and scattering is given by the following equation:[23]

$$\tau = -\ln(I/I_0) = (16\pi/3)R_\theta \qquad \text{Equation 8}$$

Similar to absorbance, turbidity (τ) is measured by direct transmission (I) of light through the sample of fixed pathlength. Therefore, it is an equivalent term for molar absorptivity but only in the case of non-absorbing species. Turbidity measurements are often performed using a UV spectrometer at wavelengths in the range of 350 – 600 nm.

Since turbidity depends on the loss of light due to scattering, it can be mathematically related to the molecular weight of the scattering species by using the following equation (similar to the Rayleigh scattering equation 4):[17,22,23]

$$\frac{Hc}{\tau} = \frac{1}{M_w} + 2B_2c \qquad \text{Equation 9}$$

where H is a constant and related to the optical constant K by the following equation:

$$H = \frac{16\pi K}{3} = \frac{32\pi^3 n_0^2}{3N_A\lambda_0^4}\left(\frac{dn}{dc}\right)^2 \qquad \text{Equation 10}$$

Change in turbidity of protein solutions is also used as a measure of protein aggregation.[38,39] Mahler et al.[39] studied the effect of stirring and shaking on the aggregation of an antibody with and without polysorbate 80 using turbidity measurements (at 350 and 550 nm). Turbidity increased on stirring the samples (without polysorbate 80) over extend period of time indicating

the formation of protein aggregates. However, in the presence of polysorbate 80, turbidity of the protein samples did not increase significantly even after 48 hours of stirring or shaking.

5. CORRELATION BETWEEN DILUTE SOLUTION PROPERTIES AND HIGH CONCENTRATION BEHAVIOR

All the SLS techniques discussed so far are limited to characterizing RSA and aggregation under low protein concentrations. The dilute solution properties are used to predict the behavior of proteins at high concentration. In a study by Kumar et al.,[21] effect of ionic strength on aggregation propensity of a bispecific MAb was studied at low (5 mg/mL) and high (100 mg/mL) concentrations. Change in protein-protein interactions was characterized by B_2 values obtained from SLS studies under dilute conditions (0 – 10 mg/mL). 5 and 100 mg/mL protein solutions at different ionic strength conditions were heated at 40 ºC for 21 days to induce aggregation. After heating, the amount of aggregates was measured in the samples. The results showed that for dilute 5 mg/mL samples, minimum aggregation was observed at conditions where B_2 values were more positive. However, for high concentration (100 mg/mL) samples the aggregation propensity did not correlate well with dilute solution properties (B_2 values). This and other literature reports[20,27] have indicated that the high concentration behavior of proteins can be different than predicted using dilute solution properties. When using techniques that characterize proteins at low concentrations, one should be cautious of extrapolating the results to higher concentrations.

6. SUMMARY AND CONCLUDING REMARKS

One of the major challenges faced during high concentration protein formulation is the ability to identify the solution properties that can cause protein instability (such as reversible

self-association and aggregation) in the early development stage. Light scattering continues to be the most used technique for characterizing molecular interactions, reversible self-association and aggregation in protein solutions. SLS techniques have been used either in a low-throughput batch mode under dilute protein concentrations (0 – 10 mg/mL) or in line with SEC. The major drawback is that on dilution the information about concentration based RSA and/or aggregation of proteins goes undetected.

UV light scattering technique has the potential to characterize RSA and aggregation in protein solutions. UV wavelengths for example 350 nm, can be used to characterize particles with a size less than 17.5 nm ($\lambda_0/20$). This is beneficial because the scattering intensity increases with the decrease in wavelength to the power four making it a very sensitive to changes in the size of the proteins in solution.

7. REFERENCES

1. Aggarwal, S. R. What's fueling the biotech engine-2012 to 2013. *Nat. Biotechnol.* **2014**, *32*, 32-39.

2. Carlson, R. Estimating the biotech sector's contribution to the US economy. *Nat Biotech* **2016**, *34*, 247-255.

3. Aggarwal, S. What's fueling the biotech engine? *Nat. Biotechnol.* **2007**, *25*, 1097-1104.

4. Aggarwal, S. What's fueling the biotech engine - 2007. *Nat. Biotechnol.* **2008**, *26*, 1227-1233.

5. Aggarwal, S. What's fueling the biotech engine-2009-2010. *Nat. Biotechnol.* **2010**, *28*, 1165-1171.

6. Aggarwal, S. What's fueling the biotech engine-2010 to 2011. *Nat. Biotechnol.* **2011**, *29*, 1083-1089.

7. Aggarwal, S. What's fueling the biotech engine-2011 to 2012. *Nat. Biotechnol.* **2012**, *30*, 1191-1197.

8. Wang, W. Protein aggregation and its inhibition in biopharmaceutics. *Int. J. Pharm.* **2005**, *289*, 1-30.

9. Shire, S. J.; Shahrokh, Z.; Liu, J. Challenges in the development of high protein concentration formulations. *J. Pharm. Sci.* **2004**, *93*, 1390-1402.

10. Goswami, S.; Wang, W.; Arakawa, T.; Ohtake, S. Developments and Challenges for mAb-Based Therapeutics. **2013**, *2, 452-500*.

11. Philo, J. S. Is any measurement method optimal for all aggregate sizes and types? *The AAPS Journal* **2006**, *8*, E564-E571.

12. Knobloch, J. E.; Shaklee, P. N. Absolute Molecular Weight Distribution of Low-Molecular-Weight Heparins by Size-Exclusion Chromatography with Multiangle Laser Light Scattering Detection. *Analytical Biochemistry* **1997**, *245*, 231-241.

13. Wyatt, P. J. Light scattering and the absolute characterization of macromolecules. *Analytica Chimica Acta* **1993**, *272*, 1-40.

14. Wyatt, P. J. Multiangle light scattering: The basic tool for macromolecular characterization. *Instrum Sci Technol* **1997**, *25*, 1-18.

15. Nguyen, L. T.; Wiencek, J. M.; Kirsch, L. E. Characterization Methods for the Physical Stability of Biopharmaceuticals. *PDA J. Pharm. Sci. Technol.* **2003**, *57*, 429-445.

16. Oliva, A.; Llabrés, M.; Fariña, J. B. Applications of multi-angle laser light-scattering detection in the analysis of peptides and proteins. *Curr Drug Discov Technol* **2004**, *1*, 229-242.

17. Holtzer, A. Light-scattering in physical chemistry. K. A. Stacey, Academic Press, New York, 1956. 230 pp. $6.50. *Journal of Polymer Science* **1958**, *33*, 527-528.

18. Zimm, B. H. Apparatus and methods for measurement and interpretation of the angular variation of light scattering; Preliminary results on polystyrene solutions. *J. Chem. Phys.* **1948**, *16*, 1099-1116.

19. Debye, P. P. A photoelectric instrument for light scattering measurements and a differential refractometer. *J. Appl. Phys.* **1946**, *17*, 392-398.

20. Chari, R.; Jerath, K.; Badkar, A. V.; Kalonia, D. S. Long- and short-range electrostatic interactions affect the rheology of highly concentrated antibody solutions. *Pharm. Res.* **2009**, *26*, 2607-2618.

21. Kumar, V.; Dixit, N.; Zhou, L.; Fraunhofer, W. Impact of short range hydrophobic interactions and long range electrostatic forces on the aggregation kinetics of a monoclonal antibody and a dual-variable domain immunoglobulin at low and high concentrations. *Int. J. Pharm.* **2011**, *421*, 82-93.

22. Paul C. Hiemenz, Raj Rajagopalan. Chpt5. Static and dynamic light scattering and other radiation scattering. In *Principles of Colloid and Surface Chemistry*CRS Press: Boca Raton, FL, **1997**; pp 193-244.

23. Tanford, C. *Physical chemistry of macromolecules. Inc;* John Wiley & Sons, Inc.: New York, **1961**; Vol. 51, pp 190-190.

24. Neal, B. L.; Asthagiri, D.; Velev, O. D.; Lenhoff, A. M.; Kaler, E. W. Why is the osmotic second virial coefficient related to protein crystallization? *J. Cryst. Growth* **1999**, *196*, 377-387.

25. Curtis, R. A.; Prausnitz, J. M.; Blanch, H. W. Protein-protein and protein-salt interactions in aqueous protein solutions containing concentrated electrolytes. *Biotechnol. Bioeng.* **1998**, *57*, 11-21.

26. Curtis, R. A.; Ulrich, J.; Montaser, A.; Prausnitz, J. M.; Blanch, H. W. Protein-protein interactions in concentrated electrolyte solutions: Hofmeister-series effects. *Biotechnol. Bioeng.* **2002**, *79*, 367-380.

27. Saluja, A.; Kalonia, D. S. Nature and consequences of protein-protein interactions in high protein concentration solutions. *Int. J. Pharm.* **2008**, *358*, 1-15.

28. Yadav, S.; Liu, J.; Scherer, T. M.; Gokarn, Y.; Demeule, B.; Kanai, S.; Andya, J. D.; Shire, S. J. Assessment and significance of protein-protein interactions during development of protein biopharmaceuticals. *Biophysical Reviews* **2013**, *5*, 121-136.

29. Abbas, S. A.; Sharma, V. K.; Patapoff, T. W.; Kalonia, D. S. Characterization of antibody-polyol interactions by static light scattering: Implications for physical stability of protein formulations. *Int. J. Pharm.* **2013**, *448*, 382-389.

30. Minton, A. P. Static light scattering from concentrated protein solutions, I: General theory for protein mixtures and application to self-associating proteins. *Biophys. J.* **2007**, *93*, 1321-1328.

31. Fernández, C.; Minton, A. P. Static light scattering from concentrated protein solutions II: Experimental test of theory for protein mixtures and weakly self-associating proteins. *Biophys. J.* **2009**, *96*, 1992-1998.

32. Esfandiary, R.; Hayes, D. B.; Parupudi, A.; Casas-finet, J.; Bai, S.; Samra, H. S.; Shah, A. U.; Sathish, H. A. A systematic multitechnique approach for detection and characterization of reversible self-association during formulation development of therapeutic antibodies. *J. Pharm. Sci.* **2013**, *102*, 62-72.

33. Bajaj, H.; Sharma, V. K.; Kalonia, D. S. A high-throughput method for detection of protein self-association and second virial coefficient using size-exclusion chromatography through simultaneous measurement of concentration and scattered light intensity. *Pharm. Res.* **2007**, *24*, 2071-2083.

34. Li, Y.; Weiss IV, W. F.; Roberts, C. J. Characterization of high-molecular-weight nonnative aggregates and aggregation kinetics by size exclusion chromatography with inline multi-angle laser light scattering. *J. Pharm. Sci.* 2009, *98*, 3997-4016.

35. Amin, S.; Barnett, G. V.; Pathak, J. A.; Roberts, C. J.; Sarangapani, P. S. Protein aggregation, particle formation, characterization & rheology. *Curr. Opin. Colloid Interface Sci.* **2014**, *19*, 438-449.

36. Wyatt, P. J. The story of MALS. *Am. Lab.* **2013**, *45*.

37. Chen, K.; Kromin, A.; Ulmer, M. P.; Wessels, B. W.; Backman, V. Nanoparticle sizing with a resolution beyond the diffraction limit using UV light scattering spectroscopy. *Opt. Commun.* **2003**, *228*, 1-7.

38. Parker, T. G.; Dalgleish, D. G. The use of light-scattering and turbidity measurements to study the kinetics of extensively aggregating proteins: αs-Casein. *Biopolymers* **1977**, *16*, 2533-2547.

39. Mahler, H.; Müller, R.; Frieβ, W.; Delille, A.; Matheus, S. Induction and analysis of aggregates in a liquid IgG1-antibody formulation. *European Journal of Pharmaceutics and Biopharmaceutics* **2005**, *59*, 407-417.

8. FIGURES

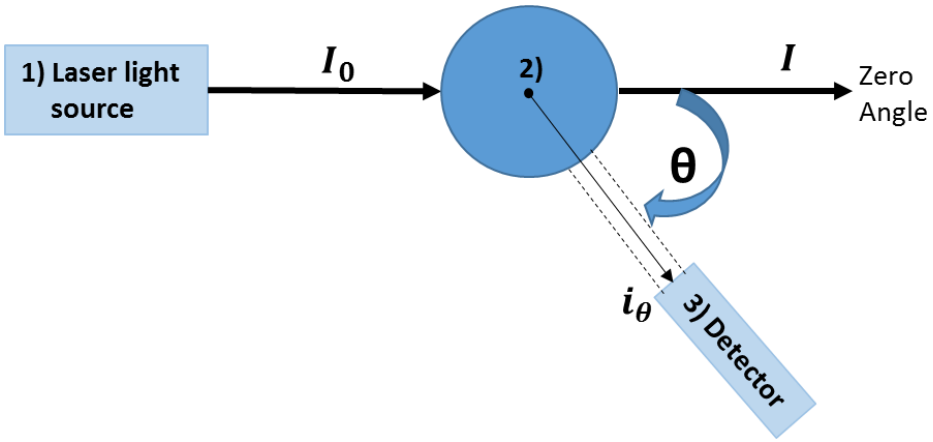

Figure 1. Static light scattering spectrometer. 1) Laser light source, 2) sample holder and 3) detector

-

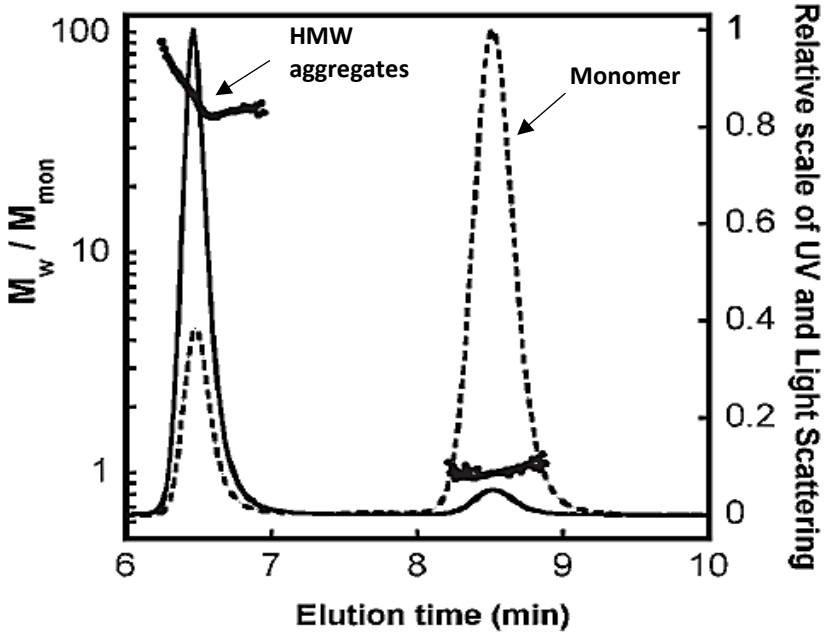

Figure 2. SEC-MALS chromatogram and M_w profile for α-chymotrypsinogen A taken from Li et al. 2009. Solid and dotted lines, respectively, represent relative light scattering intensity (secondary y-axis, only 90º scattering intensity) and relative UV absorbance at 280 nm (secondary y-axis). M_w values (scaled by M_{mon}) of the two peaks are given by symbols (primary y-axis).

Chapter 3

Effect of Absorbance on Light Scattering and Turbidity of Protein Solutions

CONTENTS

Chapter 3

1. ABSTRACT

The objective of this work is to investigate the contribution of effect of absorption on Rayleigh light scattering and turbidity of proteins in the ultraviolet (UV) region. UV region has contributions from both chromophoric absorption (I_A) and scattering (I_S) of light. Molecules that absorb (tyrosine), scatter (starch), and absorb and scatter simultaneously (tyrosine-starch mixtures, proteins) were used. Based on the absorption scans of tyrosine and proteins the wavelengths studied are divided into absorbing (260 – 310 nm) and non-absorbing (310 – 350 nm) region. Scattering intensities for pure tyrosine were negligible compared to pure starch at all the wavelengths. For tyrosine-starch mixtures, the 90º scattering intensities of starch samples decreased in the tyrosine absorbing region, however, remained unchanged in the non-absorbing region. The 90º scattering intensity of proteins in non-absorbing regions increased as a function of protein concentration. Whereas, at 280 nm (absorption maximum) 90º scattering intensity was affected by concentration, molecular weight and molar absorptivity of the proteins. Turbidity of starch in tyrosine-starch mixtures did not depend on tyrosine concentration. These findings suggest that the decrease in scattering intensity observed at 280 nm for starch-tyrosine mixtures, BSA and protein X is because of the reabsorption of scattered light by absorbing chromophores.

2. **KEYWORDS:** UV light scattering, Rayleigh light scattering, protein absorption, turbidity

CHEMICAL COMPOUNDS STUDIES IN THIS ARTICLE

L-tyrosine (PubChem CID: 6057); Hydroxyethyl starch (PubChem CID: 16213095); Bovine serum albumin

ABBREVIATIONS

OD, Optical density;

LS, light scattering;

HES, hydroxyethyl starch;

BSA, bovine serum albumin;

GDH, glutamate dehydrogenase;

MAbs, monoclonal antibodies

3. INTRODUCTION

Static light scattering (SLS) has been used as a method to characterize molecular weight, nonideality (second virial coefficient, B_{22}) and size of macromolecules under dilute solution conditions.[1-6] It is a rapid and non-destructive technique that requires small sample volume (< 60 uL) for analysis. The commercially available scattering instruments have laser light sources ranging from 560 – 650 nm wavelength range. Rayleigh scattering has an inverse fourth power dependence on wavelength, i.e. higher scattering intensity at shorter wavelengths.[7,8] Therefore, the range and sensitivity of this technique can be extended by using shorter wavelengths in the ultraviolet range.

In the UV range proteins absorb with an absorption maximum around 278-280 nm (known as λ_{max}). The absorption for proteins in the UV region is due to the contributions from four chromophoric groups: side chains of tryptophan (Trp), tyrosine (Tyr), phenylalanine (Phe) and disulfide bonds (cystines).[9-12] The absorbance is used to calculate the sample concentration by applying the Beer-Lambert law: A = εcl, where A is the absorbance, ε is the molar absorptivity (1/M.cm), c is the concentration (M) and l is the pathlength (cm).[10,13] Accordingly, absorbance varies linearly with pathlength and concentration of the absorbing molecule. The Beer-Lambert law assumes that when the light passes through a continuous sample of non-interacting molecules, a fraction of the light is absorbed and the remaining light is transmitted. For large molecules (proteins, DNA, viruses etc.), the spectrometer records the extinction of light due to both absorption and scattering, resulting in a deviation from the Beer-Lambert law.[14] When the light reaching the detector is attenuated due to absorption by protein chromophores and light scattering, the logarithmic ratio of incident (I_0) to transmitted intensity (I_T) is referred to as optical density ($\mathrm{OD} = \log(I_0/I_T)$). Absorption is the light attenuation because of the presence of

chromophores only. Turbidity (τ) is the ratio of total light scattered in all directions to the incident light intensity. The mathematical relationships are discussed later in this chapter.

The effect of scattering contribution to the absorption spectra of proteins has been studied extensively to determine concentration, molar absorptivity and evaluate structural changes in proteins. However, there are no reports on the effect of UV absorbance on light scattering in protein solutions. The focus of this work is to investigate the effect of absorbing species on Rayleigh light scattering and turbidity of tyrosine, starch and proteins. The work is further extended to evaluate the effect of concentration, absorption coefficient and molecular weight of the protein on the scattering intensity.

4. EXPERIMENTAL SECTION

4.1. Materials

All chemicals and buffer reagents used were of highest purity and were purchased from commercial sources. Bovine serum albumin (BSA), hydroxyethyl starch (HES) and L-tyrosine (Tyr) were obtained from Sigma-Aldrich (St. Louis, Missouri) and were used without further purification. The molecular weight used for BSA and Tyr are ~67 kDa and 181.19 Da respectively. Protein X, a monoclonal antibody of molecular weight 149 kDa was also used. The buffer reagents obtained from Fisher Scientific (Fair Lawn, NJ, USA) were glacial acetic acid-sodium acetate for pH 5 and monobasic-dibasic sodium phosphate for pH 7.0.

4.2. Methods

4.2.1. Sample Preparation

Tyrosine (~0.33 mg/mL) and HES (1% w/v) stocks were prepared by weighing the required amount in a volumetric flask and triple distilled water was added (q.s.) to make up the

volume. Tyrosine stock was filtered using 0.22 μm syringe filter to remove foreign particles. Samples of 0.02, 0.04 and 0.08 mg/mL tyrosine concentration were made by volumetric dilution of the stock. The pH of tyrosine samples was noted to be around 5.8. HES samples of 0.02, 0.04, 0.06, 0.08, and 0.10 % w/v were also made by volumetric dilution of the stock.

The buffers were prepared at the required ionic strength by dissolving the desired buffer salts in triple distilled water. The buffer pHs (if needed) were adjusted using 1 N HCl or NaOH and filtered using a 0.1 μm filter (Milipore, MA, USA). BSA stock solution was prepared by weight, by dissolving the required amount in pH 5 acetate buffer. BSA samples of 0.1, 0.2, 0.5, 1 and 2 mg/mL were made by serial dilution of the stock. Protein X stocks were prepared by multiple buffer exchange cycles in the desired buffer. Allegra X-15R centrifuge (Beckman Coulter, Indianapolis, IN) and Amicon Ultra centrifugation dialysis tubes (Millipore, Billerica, MA), with 10 kDa MWCO were used for buffer exchange. Four to six buffer exchange cycles were performed at 3000 rcf and 10 °C. At the end of dialysis, the pH of the protein stock was checked to ensure it was within $\pm$ 0.05 of the target value and concentrations were measured using Solo VPE (C Technologies Inc., Bridgewater, NJ) and performing buffer corrections. Protein A samples of 0.2, 0.4 and 1 mg/mL were prepared by serial dilution of the stock

4.2.2. Light Scattering (LS) Studies

Light scattering measurements were done using Perkin Elmer Luminescence Spectrofluorometer, Model LS50. LS 50 has a xenon flash lamp as a light source with a wavelength range of 200 – 1100 nm. LS intensity was measured at a 90° angle to the incident light source with excitation and emission monochromators both set to the same wavelength. A four window, 500-650 μL sample volume quartz cuvette was used for all the measurements. Since the intensity of xenon flash lamp source in this spectrometer shows a wavelength

dependence, light scattering intensities were plotted as sample to solvent ratios. For tyrosine-starch mixtures, wavelengths of incident light used were 260 – 290 (at an interval of 5 nm) and 290 – 360 (at an interval of 10 nm). For BSA, scattering intensities were measured from 260 – 360 nm (at an interval of 1 nm). These wavelengths were chosen because in 320-360 nm region optical density is measured and extrapolated to calculate LS contribution at 280 nm (wavelength of absorption maxima for proteins).

4.2.3. UV-Vis Absorption Studies

UV- Vis absorption and % transmittance scans were performed at a scan rate of 60 nm/min using Cary 50-Bio UV-Vis spectrophotometer (Varian Inc., CA, USA). Path length of 1 cm was used. Absorption scans for all the samples were taken to determine their optical density contribution in the region of 260 – 350 nm. Divided rectangular cuvette from Starna Cells (Atascadero, CA) was used for studying effect of absorption on turbidity of tyrosine-starch mixtures. The absorption coefficients used for tyrosine, BSA and Protein X are 8.17,[15] 0.66[16] and 1.5 ml/mg*cm, respectively.

5. RESULTS

5.1. Effect of Absorption on 90º Scattering Intensity

5.1.1. Light Scattering studies for individual tyrosine and starch solutions

Figure 1 shows the changes in scattering intensity ratios (tyrosine to water) as a function of tyrosine concentration at 270 and 350 nm. Tyrosine solutions showed negligible change in the scattering intensity ratios at 350 nm. However, at 270 nm (i.e. the absorbing wavelength of chromophore) the scattering intensity decreased with an increase in the tyrosine concentration.

Figure 2 shows the changes in light scattering intensity ratios (starch to buffer) as a function of starch concentration at different wavelengths (280, 320 and 350 nm). The scattering intensity for starch solutions increased non-linearly with an increase in starch concentration at each wavelength studied. The scattering intensity ratios were higher at 280 nm compared to 320 and 350 nm at each starch concentration. For example, the scattering intensity ratio was 23.7 at 280 nm, 16.4 at 320 nm and 15 at 350 nm. The difference in scattering intensity ratios measured at 320 and 350 nm was significant only at concentrations of 0.08 and 0.1% w/v starch.

5.1.2. Light Scattering studies for tyrosine-starch mixtures

Figure 3 shows the change in light scattering intensity ratios (starch-tyrosine mixtures to starch) and absorbance (of tyrosine samples) as a function of wavelength of incident light measured in the range of 260 – 360 nm. The light scattering intensities were measured for 0.1% w/v starch samples before and after addition of 0.04 (blue triangles), 0.08 (red triangles) and 0.12 (black triangles) mg/mL tyrosine. Based on the absorptions spectra of tyrosine (shown by blue solid line, red dash line and black dash-dot line) the wavelength range is divided into absorbing and non-absorbing region. In the non-absorbing region of 300 – 360 nm, the light scattering intensity ratios were close to 1 and the absorption of tyrosine samples was negligible. However, in the absorbing region of 260-290 nm wavelength range, the absorption intensity of tyrosine samples increased with an increase in tyrosine concentration. The peak for absorption maximum was measured at 275 nm. In the non-absorbing region, the scattering intensity ratios for tyrosine-starch mixtures decreased to a value of less than 1. At each wavelength, the scattering intensity for tyrosine-starch mixture decreased with increase in tyrosine concentration. For examples, at 275 nm the scattering intensity ratios for mixture containing 0.04 mg/mL tyrosine was 0.49, 0.08 mg/mL tyrosine was 0.23, and 0.12 mg/mL tyrosine was 0.12. The scatter intensity ratio plots as

a function of wavelength followed an inverted trend compared to their corresponding tyrosine absorption spectra.

5.1.3. Light Scattering Studies for BSA (~67 KDa, absorption maxima around 280 nm)

Figure 4 shows (A) optical density and (B) light scattering intensity ratios (of sample to buffer) and percent transmittance (of samples) as a function of wavelength for 0.1, 0.2, 0.5, 1.0 and 2.0 mg/mL BSA samples prepared in pH 5 acetate buffer. Based on the absorptions spectra of BSA the wavelength range is divided into absorbing (260 – 310 nm) and non-absorbing region (310 – 350 nm). As shown in figure 4A at non-absorbing wavelengths the OD contribution was negligible for 0.1, 0.2 and 0.5 mg/mL as compared to that of 1.0 and 2.0 mg/mL BSA. In the absorbing region, the OD for BSA increased with increase in BSA concentration and absorption maximum was seen around 280 nm. As shown in figure 4B at non-absorbing wavelengths the scattering intensity ratio followed the concentration trends, showing an increase in LS intensity with an increase in BSA concentration. The percent transmittance in this region followed the inverse concentration trend and a decrease in percent transmittance was observed with an increase in BSA concentration. The increasing order of LS intensity based on concentration was as follows: 0.1 < 0.2 < 0.5 < 1.0 < 2.0 mg/mL BSA. However, at the absorbing wavelengths the scattering intensities did not show an increase with increase in BSA concentration. The trend for scattering intensity ratio was opposite at 280 nm in comparison to 350 nm. For example, the LS intensity ratio was lowest at 280 nm (absorption maxima) whereas, it was highest at 350 nm for 2.0 mg/mL BSA compared to other concentrations. The increasing order of LS intensity based on concentration at 280 nm was as follows: 2.0< 0.1 < 0.2 < 0.5 = 1.0 mg/mL BSA.

5.1.4. Light Scattering Studies for Protein X (~149 kDa, absorption maxima around 280 nm)

Figure 5 shows the change in scattering intensity ratio (protein to buffer) and percent transmittance (of protein X samples) as a function of wavelength for 0.2, 0.4 and 1 mg/mL protein X concentrations. In the non-absorbing region for protein X (i.e. 320 – 350 nm) the scattering intensity increased with an increase in the protein concentration. At each wavelength in this range the scattering intensity was highest for 1 mg/mL protein X followed by 0.4 and 0.2 mg/mL. However, the region where protein X had significant absorption (i.e. 260 – 310 nm), the scattering intensity ratio did not follow a concentration trend. At 280 nm (wavelength of absorption maximum) the light scattering intensity ratio was lowest for 1 mg/mL protein X.

5.2. Effect of Absorption on Turbidity and Optical Density

The effect of absorption on turbidity and optical density was studies using a divided rectangular cuvette shown in figure 6. The starch and tyrosine samples were pipetted in cell 1 and 2, respectively. Absorption scan 1 was obtained by aligning the cuvette such that cell 1 faced the light source and cell 2 faced the detector. In this alignment the light was first passed through a scattering (starch) medium followed by an absorbing (tyrosine) medium. Absorption scan 2 was obtained by rotating the cuvette by 180 degree such that the light first passes through the absorbing tyrosine medium followed by scattering starch solution. Figure 7 shows the absorption spectra collected for 0.2% starch in cell 1 and 0.20 mg/mL tyrosine in cell 2. The absorption scan 1 and scan 2 did not have any major differences. The same observation was noted for all other samples as well. Thereby, for visual simplicity only one representative scan for each sample is shown in figure 8. Figure 8 shows the absorption spectra for starch, tyrosine and starch-tyrosine mixtures obtained using the divided rectangular cuvette (shown in figure 6).

A fixed 0.2% w/v concentration of starch with 0.12, 0.20 and 0.25 mg/mL tyrosine were studied. The solid lines are absorption spectra for pure tyrosine in cell 1 and water in cell 2. Dash-dot-dot line represents spectra obtained by placing 0.2% w/v starch and water in cell 1 and 2, respectively. The dashed line represents starch-tyrosine mixture in cell 1 and water in cell 2. The dotted lines represent the absorption spectra obtained by placing tyrosine and starch in cell 1 and 2, respectively. In 240 – 300 nm range (absorbing wavelengths) tyrosine absorbs significantly giving an absorption maximum around 275 nm. The maximum absorption intensity increased with increase in tyrosine concentrations. In the presence of 0.2% w/v starch, the maximum absorption intensity was higher at each tyrosine concentration. However, the absorption spectra did not show a significant difference for scans of tyrosine starch mixtures in cell 1 compared to when tyrosine and starch were each in different cells.

6. DISCUSSION

For the purposes of this study, molecules were selected based on their interactions with light: molecules that only absorb light (Tyr), only scatter light (starch), and simultaneously absorb and scatter light (tyrosine-starch mixtures, high molecular weight peptides, proteins, MAbs).

For molecules only undergoing absorption, the sample absorbance (A) is a logarithmic ratio of incident (I_0) to transmitted (I) intensity and is directly proportional to the absorption coefficient (a_{abs}, mL/(mg*cm)), concentration (c, mg/mL) and path length (l, cm), given by the Beer Lambert law:[13]

$$A = \log\left({}^{I_0}/_{I}\right) = a_{abs}cl \qquad \text{Equation 1}$$

For any given molecule a_{abs} is an intrinsic property and is independent of the concentration.

For non-absorbing molecules that only scatter light, the scattering intensity (i_s) per unit volume is given by following equation:[7,8]

$$i_s = K(1 + cos^2\theta)I_0 wM/r^2 \qquad \text{Equation 2}$$

where θ is the scattering angle, I_0 is the initial intensity of unpolarized light source, r is the distance between scattering molecule and detector, w and M are concentration (g/mL) and molecular weight of the scattering molecule, respectively and

$$K = \frac{2\pi^2 n_0^2}{N_A \lambda_0^4}\left(\frac{dn}{dc}\right)^2$$

The optical constant K depends on the solution refractive index (n_0), Avogadro's number (N_A), wavelength of incident light (λ_0) and change in refractive index of the scattering molecule (dn/dc). Turbidity (τ) is the total light scattered in all the directions and is obtained by integrating the scattering intensity over the volume of sphere as shown by the following equation:[7,20]

$$\tau = 2\pi R_\theta I_0 \int_{\theta=0}^{\pi}(1 + cos^2\theta)\sin\theta\, d\theta = \frac{16\pi}{3} R_\theta \qquad \text{Equation 3}$$

where Rayleigh ratio, $R_\theta = r^2 i_s/(1 + cos^2\theta)I_0$. This equation is valid only under dilute solution conditions for solutes that behave as hard spheres with radius $< \lambda_0/20$. The scattering intensity, i_s was measured using spectrofluorometer at a fixed angle i.e. 90º for this study. Turbidity, however, is the intensity of light attenuated due to scattering in all directions and was measured at 180º angle using a UV spectrometer.

6.1. 90º Light Scattering Studies for tyrosine, starch and tyrosine-starch mixtures

Figure 1 shows scattering intensity for pure tyrosine samples as a function of concentration. At 350 nm (non-absorbing wavelength), tyrosine scattering intensity does not change significantly with an increase in concentration because of its small size compared to the incident light. At 270 nm (absorbing wavelength), however, a decrease in scattering intensity was observed as a function of tyrosine concentration. Figure 2 shows a non-linear increase in scattering intensity of starch that has a molecular weight >200 kDa. The non-linearity was attributed to an increase in starch-starch interactions as a function of starch concentration. The increase in scattering intensity ratio of starch to buffer was higher at a shorter wavelength of incident light. The scattering intensity increase was proportional to λ^{-4} as given by the Rayleigh scattering equation.

In order to understand absorption and scattering contributions from protein molecules, tyrosine-starch mixtures were studied as model systems mimicking proteins. To interpret a relative change in light scattering intensity of starch after the addition of tyrosine, ratios of scattering intensities were plotted as a function of wavelength:

$$\frac{i_{s_2}}{i_{s_1}}(\lambda, nm) = \frac{LS\ (0.1\%\ starch + x\ mg/mL\ Tyr)}{LS\ (0.1\%\ starch)} \qquad \text{Equation 4}$$

where the subscript 1 and 2 represent light scattering (LS) intensity of starch before and after the addition of tyrosine to the sample, respectively.

Figure 3 represents the change in scattering intensity for tyrosine-starch mixtures (due to change in absorption) as a function of wavelength of incident light. Unlike tyrosine that only absorbs light and starch that only scatters; tyrosine-starch mixtures undergo both phenomena. Therefore, the scattering intensity ratio (i_{s_2}/i_{s_1}) should be 1 when absorbing species (i.e. tyrosine) has negligible effect on scattering intensity of starch. A significant deviation from the

value of 1, points to the effect of absorption on scattering intensity. In the tyrosine non-absorbing region (i.e. $\lambda > 290$ nm), the LS intensities ratios for the tyrosine-starch mixtures to starch were close to 1 at all the wavelengths of incident light (shown as blue, red and black triangles). This implied that in this wavelength region, the scattering intensity of 0.1% w/v starch was not affected by addition of different concentrations of tyrosine. However, in 260-290 nm wavelength range, the tyrosine side chain absorbs strongly giving an absorption maximum around 275 nm. In this region, the absorption intensity of tyrosine samples increased with an increase in tyrosine concentration (solid blue, dashed red and dash-dot black lines). On the other hand, the scattering intensity (i_{s_2}/i_{s_1}) ratios for tyrosine-starch mixtures decreased in the tyrosine absorption region. The decrease in scattering intensity was proportional to the increase in absorption due to tyrosine. This decrease in scattering intensity of starch shows that when absorption takes place the scattering intensity decreases and depends on the concentration of the absorbing chromophore in the solution. This could be due to one of the two reasons. First, a fraction of light is absorbed and thereby decreases the incident light available for scattering which in turn decreased the scattering intensity. Second, the scattered light is getting reabsorbed (often referred to as secondary absorption) thereby, unable to reach the detector.

6.2. 90º Light Scattering Studies for BSA and Protein X

Protein molecules absorb light (due to the presence of chromophores) and scatter light (due to its large size and molecular weight) in the UV range. In the case of tyrosine-starch mixtures the light absorption and scattering contributions were independently varied by changing the concentration of one of the species. Whereas, a change in the concentration of BSA and protein

X simultaneously affects both the light absorption and scattering, making the analysis more complex than physical mixtures of tyrosine and starch.

Figure 4 shows the absorption spectra, scattering intensity ratio (sample/buffer) and percent transmittance scans for 0.1, 0.2, 0.5, 1.0 and 2.0 mg/mL BSA samples. Based on the absorption scans, 260 – 320 nm and 320 – 350 nm are referred to as the absorbing and non-absorbing range, respectively. To understand change in scattering intensity for BSA samples in the presence and absence of absorption, two wavelengths 280 and 350 nm were used for data analysis. 280 nm is the wavelength of maximum absorption and the absorption coefficient is known, and 350 nm is a representation for scattering in the absence of absorption. At 280 nm absorption increased linearly (figure 9A) and percent transmittance (figure 9B) decreased exponentially as a function of BSA concentration. Scattering intensity (figure 9B) however, increased with BSA concentration and then decreased giving a maximum scatter intensity for 1 mg/mL BSA.

The scattering intensities at 280 nm were compared for BSA and protein X as a function of protein concentration as shown in figure 10. For BSA, maximum scatter intensity was observed around 1 mg/mL. Whereas, for protein X the maximum was observed at 0.4 mg/mL. At concentrations less than 0.4 mg/mL protein X scattering intensities were greater than BSA because of higher molecular weight of protein X (149 kDa) compared to BSA (67 kDa). At concentrations higher than 0.4 mg/mL the scattering intensity for BSA is greater than protein A because of higher absorption coefficient for protein X (1.5 mL/mg.cm) compared to BSA (0.67 mL/mg.cm).

The results show that the scattering intensity of proteins at 280 nm is a function of concentration, molecular weight and molar absorptivity. The position and height of the maximum scattering intensity depends upon the molecular weight and absorption coefficient of

proteins. At 350 nm, however, the scattering intensity only depends upon concentration and molecular weight of proteins.

6.3. Effect of Absorption on Turbidity and Optical Density

The effect of absorption on turbidity (i.e. total light scattered in all directions) was investigated using divided rectangular cell (shown in figure 6). Figure 7 shows the absorption scans obtained for starch and tyrosine. Absorption scan 1 was obtained by passing light through 0.2% w/v starch followed by 0.2 mg/mL tyrosine and then reaching the detector. Absorption scan 2 was obtained by moving the cuvette by 180º angle. Absorption scan 1 and 2 showed negligible differences in the shape or position of the absorption peak. The results show that turbidity of starch was not affected by the absorption due to tyrosine. Figure 8 compares the absorbance spectra of pure tyrosine, 0.2% w/v starch, starch-tyrosine mixtures, and starch-tyrosine in different cells. For pure tyrosine, at each concentration the absorption intensity was less than that in the presence of starch. However, the absorption spectra of starch-tyrosine mixtures, and starch-tyrosine in different cells overlapped with negligible differences. This means that the total light scattered (turbidity) does not decrease due to absorbing species unlike, the scattering intensity of starch measured at 90º angle that decreased in the presence of tyrosine. These results imply that the decrease in scattering intensity observed at 280 nm for starch-tyrosine mixtures, BSA and protein X is because of the reabsorption of scattered light by absorbing chromophores. The mathematical relationship between scattering intensity and secondary absorption is discussed in detail in section 4.4.

6.4. Relationship between 90º light scattering and secondary absorption

The results from section 6.3 indicate that decrease in scattering intensity at 280 nm is because of reabsorption of the scattered light by protein chromophores. Similar to primary absorption, secondary absorption is also a function of absorption coefficient and concentration of proteins.

Transmitted light intensity (I) is a function of absorption coefficient (a_{abs}), protein concentration (c) and pathlength (l) as given by equation (obtained by rearranging equation 1):

$$I = I_0 * 10^{-a_{abs}cl} \qquad \text{Equation 5}$$

Since scattering intensity measured at a fixed angle (i.e. 90º for this study), is the fraction of scattered light that is not reabsorbed, it can be compared to transmitted light and is a function of absorption coefficient and concentration of proteins given by the following equation:

$$i_s(measured) = i_s * 10^{-a_{abs}cl} \qquad \text{Equation 6}$$

where i_s and $i_s(measured)$ are scattering intensity of proteins before and after reabsorption, respectively. From equation 2 and 6, the intensity of scattered light measured at 280 nm is given by the following equation:

$$i_s(measured) = K(1 + cos^2\theta)I_0cM * 10^{-a_{abs}cl} \qquad \text{Equation 7}$$

The scattering intensity recorded by the 90º detector, therefore, is a function of molecular weight and absorption coefficient of proteins.

7. SUMMARY AND CONCLUSIONS

In the case of macromolecules like proteins and antibodies, UV light absorption and scattering take place simultaneously. As absorption increases, 90º Rayleigh scattering intensity decreases but turbidity does not change. Therefore, scattering intensity decreases in the presence of absorption due to reabsorption of the scattered light by the protein chromophores.

8. REFERENCES

1. Knobloch, J. E.; Shaklee, P. N. Absolute Molecular Weight Distribution of Low-Molecular-Weight Heparins by Size-Exclusion Chromatography with Multiangle Laser Light Scattering Detection. *Analytical Biochemistry* **1997***, 245*, 231-241.
2. Nguyen, L. T.; Wiencek, J. M.; Kirsch, L. E. Characterization Methods for the Physical Stability of Biopharmaceuticals. *PDA J. Pharm. Sci. Technol.* **2003***, 57*, 429-445.
3. Oliva, A.; Llabrés, M.; Fariña, J. B. Applications of multi-angle laser light-scattering detection in the analysis of peptides and proteins. *Curr. Drug Discov. Technol.* **2004***, 1*, 229-242.
4. Philo, J. S. Is any measurement method optimal for all aggregate sizes and types? *The AAPS Journal* **2006***, 8*, E564-E571.
5. Wyatt, P. J. Multiangle light scattering: The basic tool for macromolecular characterization. *Instrum. Sci. Technol.* **1997***, 25*, 1-18.
6. Wyatt, P. J. Light scattering and the absolute characterization of macromolecules. *Analytica Chimica Acta* **1993***, 272*, 1-40.
7. Tanford, C. *Physical chemistry of macromolecules. Inc;* John Wiley & Sons, Inc.: New York, **1961**, 51, 190-190.
8. Debye, P.; Bueche, A. M. Scattering by an inhomogeneous solid. *J. Appl. Phys.* **1949***, 20*, 518-525.
9. Grimsley, G. R.; Pace, C. N. Spectrophotometric Determination of Protein Concentration. In *Current Protocols in Protein Science;* John Wiley & Sons, Inc. **2001**.
10. Mach, H. Ultraviolet absorption spectroscopy. *Methods Mol. Biol.* **1995***, 40*, 91-114.
11. Mach, H.; Middaugh, C. R. Ultraviolet spectroscopy as a tool in therapeutic protein development. *J. Pharm. Sci.* **2011***, 100*, 1214-1227.
12. Pace, C. N.; Vajdos, F.; Fee, L.; Grimsley, G.; Gray, T. How to measure and predict the molar absorption coefficient of a protein. *Protein Science* **1995***, 4*, 2411-2423.
13. Skoog, D. A., *Fundamentals of analytical chemistry;* Thomson-Brooks/Cole: Australia **2004**.
14. Thakkar, S. V.; Allegre, K. M.; Joshi, S. B.; Volkin, D. B.; Middaugh, C. R. An application of ultraviolet spectroscopy to study interactions in proteins solutions at high concentrations. *J. Pharm. Sci.* **2012***, 101*, 3051-3061.
15. Kueltzo, L. A.; Middaugh, C. R. Ultraviolet Absorption Spectroscopy. In *Methods for structural analysis of protein pharmaceuticals.* Wim Jiskoot: AAPS, Arlington, VA, **2005**, 3, 1-25.
16. Weidman, P. J.; Teller, D. C.; Shapiro, B. M. Purification and characterization of proteoliaisin, a coordinating protein in fertilization envelope assembly. *J. Biol. Chem.* **1987***, 262*, 15076-15084.

17. Kerker, M. Chapter 9 - Scattering by Liquids. In *The Scattering of Light and Other Electromagnetic Radiation*; Kerker, M., Ed.; Academic Press: **1969**, 16, 487-573.
18. Scherer, T. M.; Liu, J.; Shire, S. J.; Minton, A. P. Intermolecular interactions of IgG1 monoclonal antibodies at high concentrations characterized by light scattering. *J Phys Chem B* **2010***, 114*, 12948-12957.
19. Bettelheim, F. A.; Siew, E. L. Effect of change in concentration upon lens turbidity as predicted by the random fluctuation theory. *Biophys. J.* **1983***, 41*, 29-33.
20. Eisenberg, H.; Josephs, R.; Reisler, E.; Schellman, J. A. Scattering correction to the absorbance, wavelength dependence of the refractive index increment, and molecular weight of the bovine liver glutamate dehydrogenase oligomer and subunits. *Biopolymers* **1977***, 16*, 2773-2783.

9. FIGURES

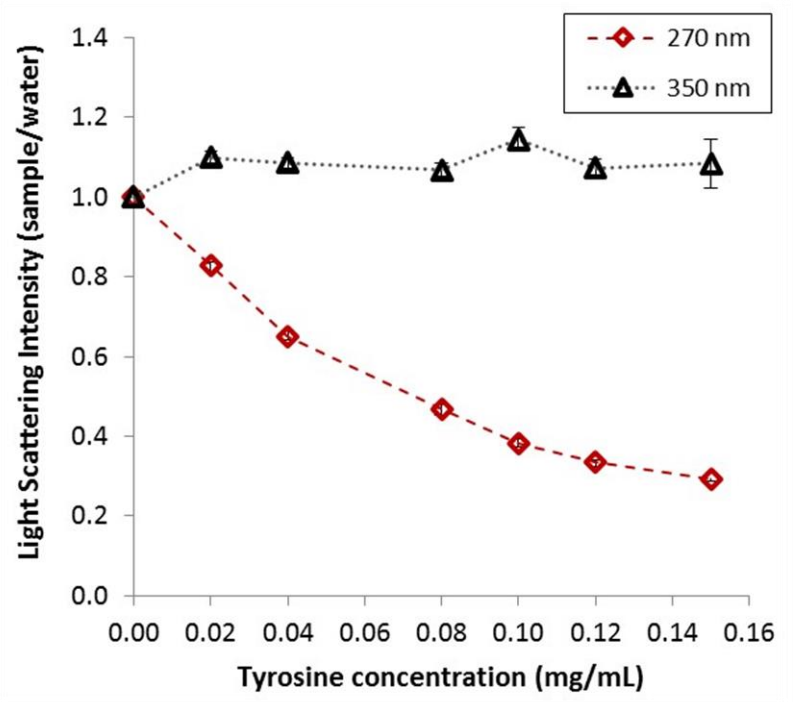

Figure 1. Light scattering intensity ratio (tyrosine/water) as a function of tyrosine concentration measured at different wavelengths of incident light: 270 (red diamonds) and 350 nm (black triangles). The lines connecting the symbols are to guide the eye and are not data points

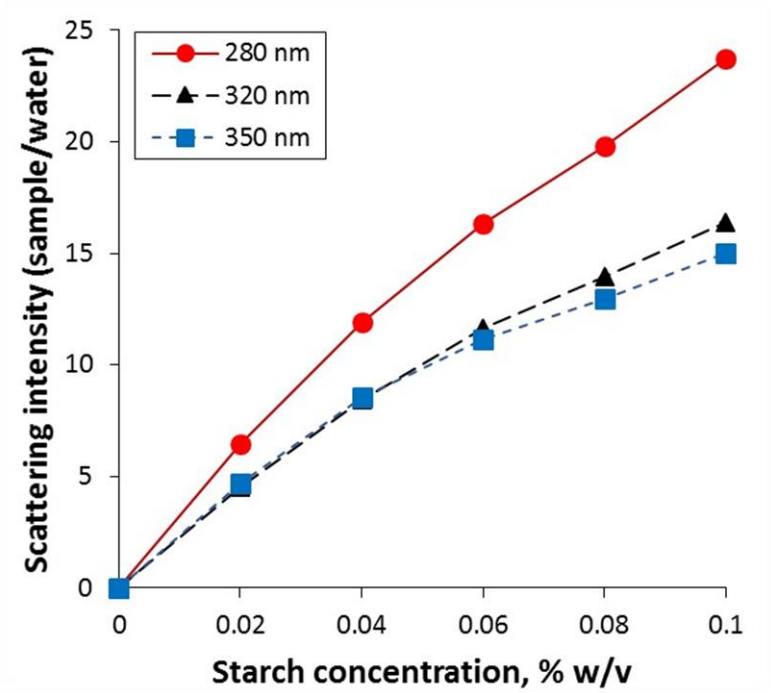

Figure 2. Light scattering intensity ratio of starch samples to water as a function of starch concentration at different wavelengths of incident light; 280 nm (red circles), 320 nm (black triangles) and 350 nm (blue squares). The lines connecting the data points are only to guide the eye and are not a result of fitting a model to the data.

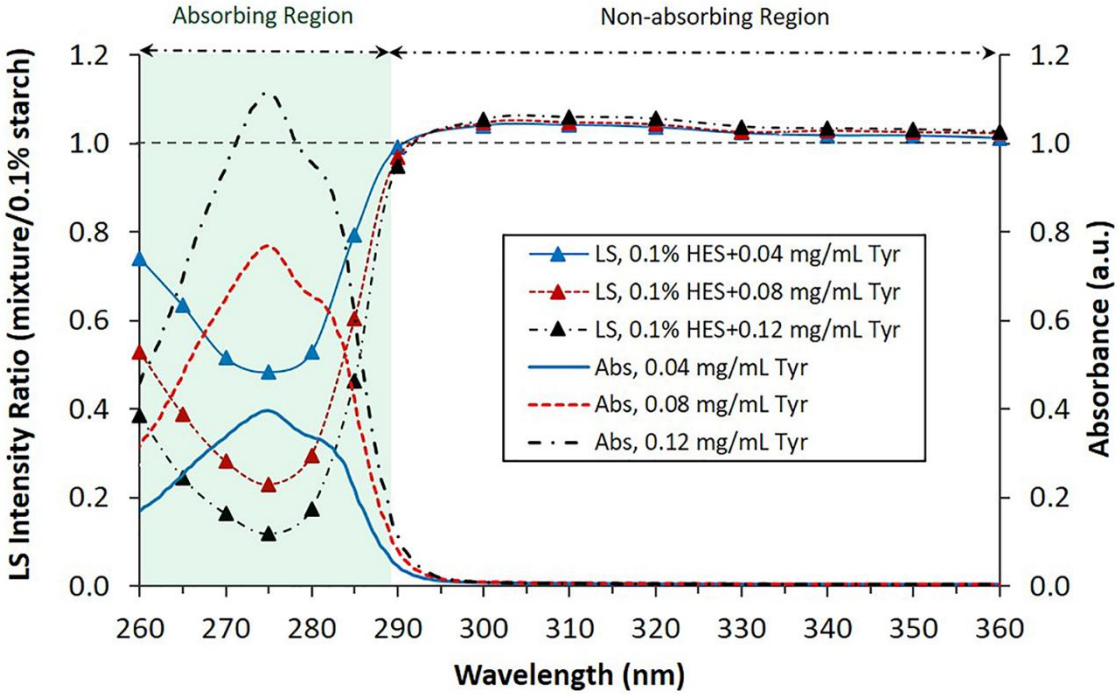

Figure 3. Light scattering intensity ratio (primary y-axis) and absorbance (secondary y-axis) as a function of wavelength of incident light. LS data is shown with symbols connected with lines and absorbance data is represented with only lines. The tyrosine-starch mixtures have 0.04 (solid blue line), 0.08 (dashed red line) and 0.12 mg/mL (dot dashed black line) of tyrosine and a fixed starch concentration of 0.1% w/v. Lines joining the symbols of LS data are to guide the eye and are not data points

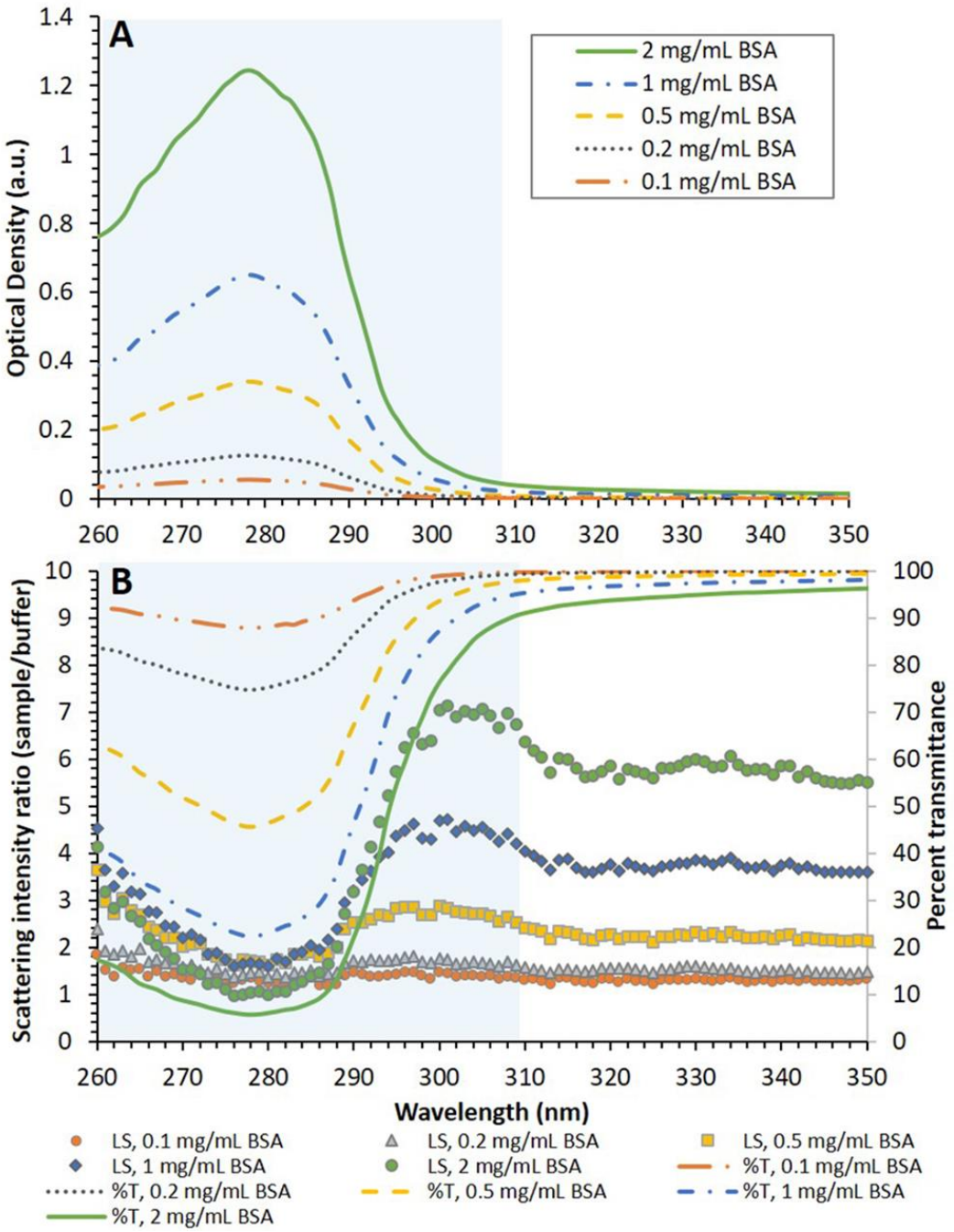

Figure 4. A. Optical density measurements and B. light scattering intensity ratios of sample to buffer (primary y-axis) and percent transmittance of BSA samples (secondary y-axis) as a function of wavelength of incident light.

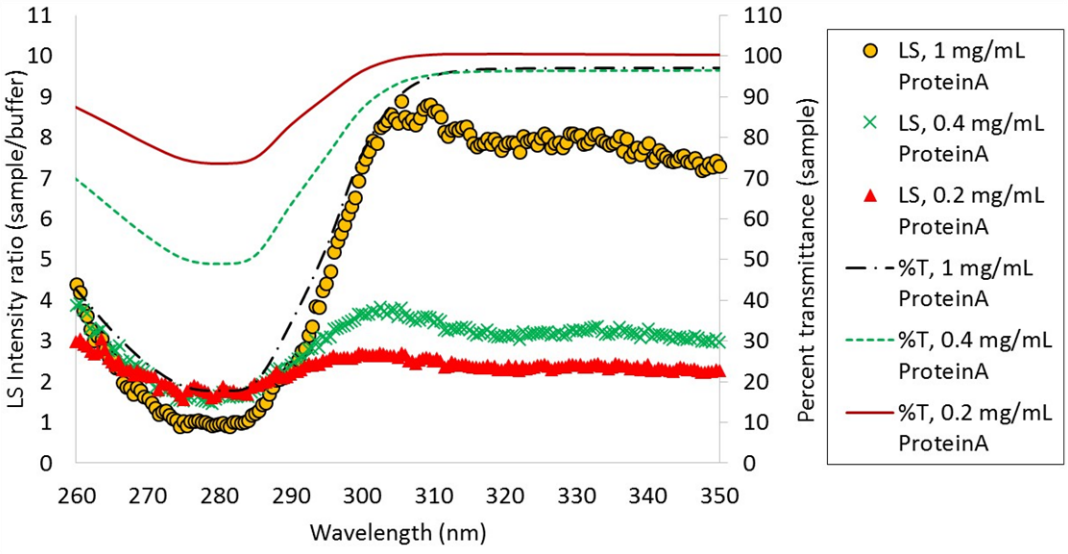

Figure 5. Light scattering intensity ratios of sample to buffer (primary y-axis) and percent transmittance of samples (secondary y-axis) as a function of wavelength of incident light for 0.2, 0.4 and 1 mg/mL protein A samples.

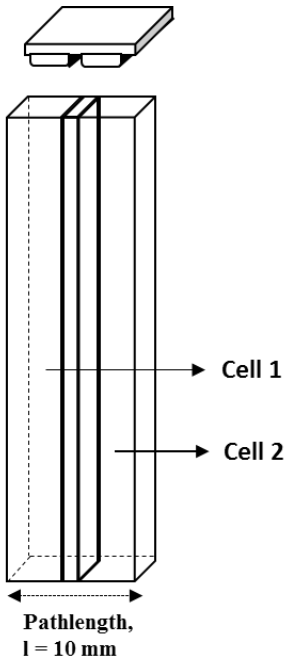

Figure 6. Divided rectangular cuvette purchased from Starna Cells (55-Q-10). It is a dual chamber cuvette, separated by a thin wall made of quartz. The optical pathlength of the cuvette is 10 mm.

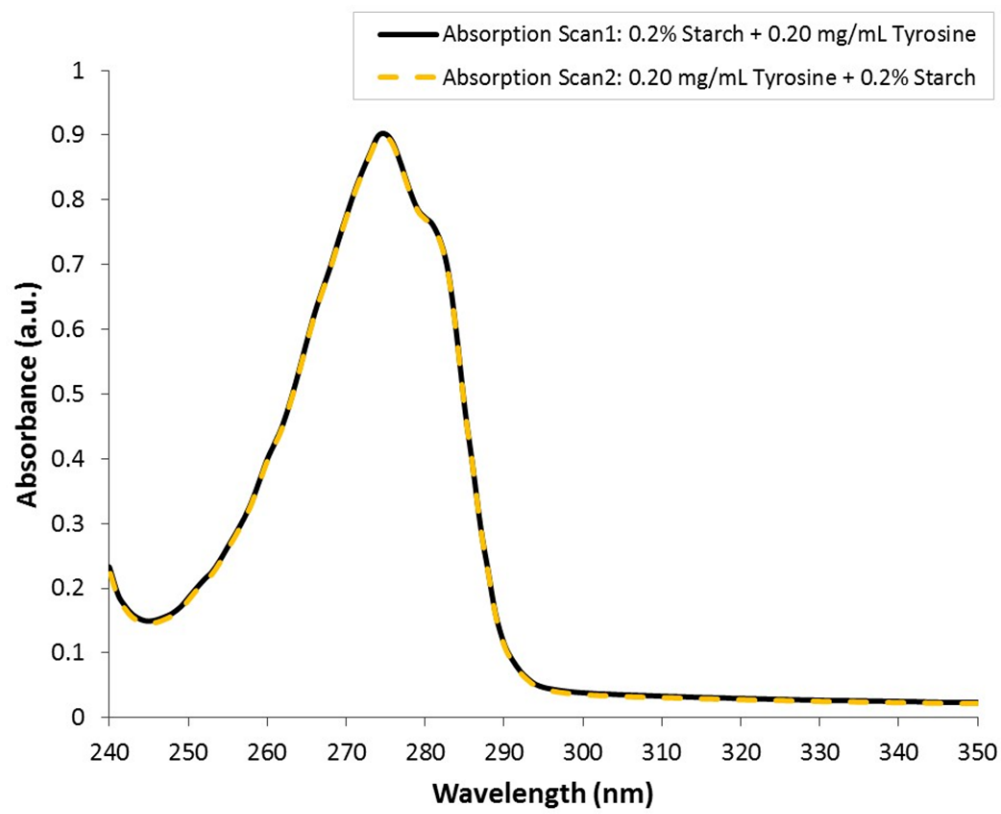

Figure 7. UV scans obtained using the divided rectangular cell. Absorption scan 1 was obtained by aligning the cuvette such that cell 1 faced the light source and cell 2 faced the detector. In this alignment the light was first passed through a scattering (0.2% w/v starch) medium followed by an absorbing (0.2 mg/mL tyrosine) medium. Absorption scan 2 was obtained by rotating the cuvette by 180 degree such that the light first passes through the absorbing tyrosine medium followed by scattering starch solution.

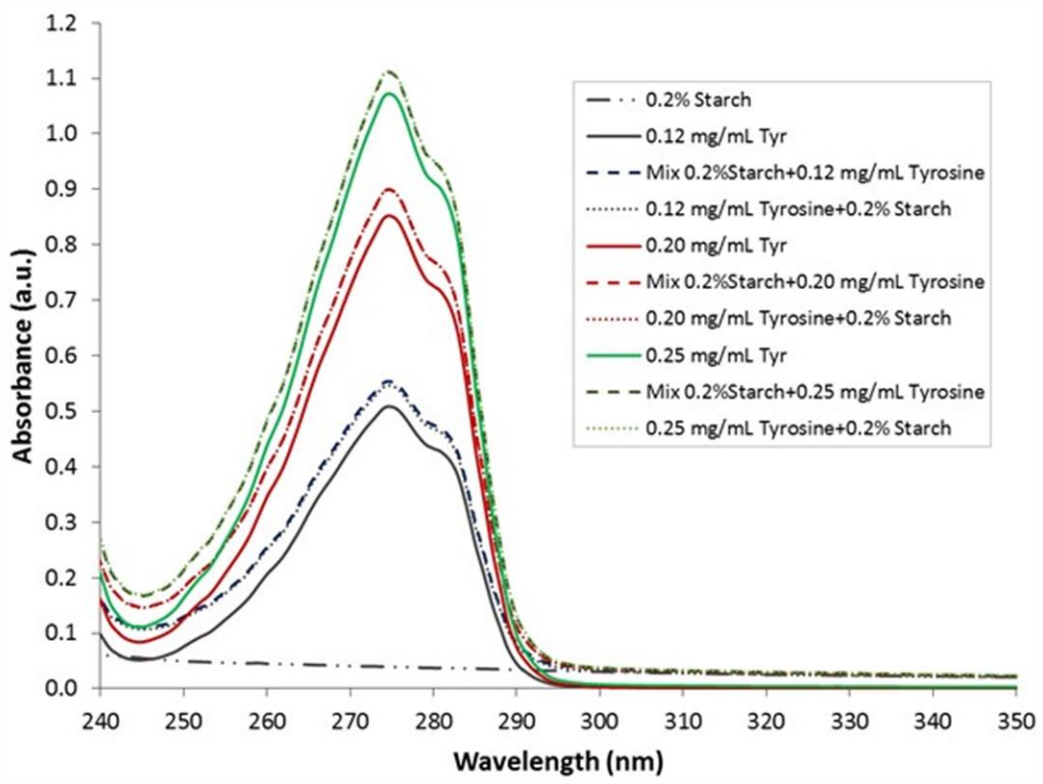

Figure 8. Absorption spectra for tyrosine, starch and starch-tyrosine mixtures. Solid line represents pure tyrosine, dash-dot-dot line represents 0.2 % w/v starch, dash line represents the tyrosine starch mixtures, and dotted line represents tyrosine (cell 1) and 0.2% w/v starch (cell 2) all measured using the divided rectangular cell.

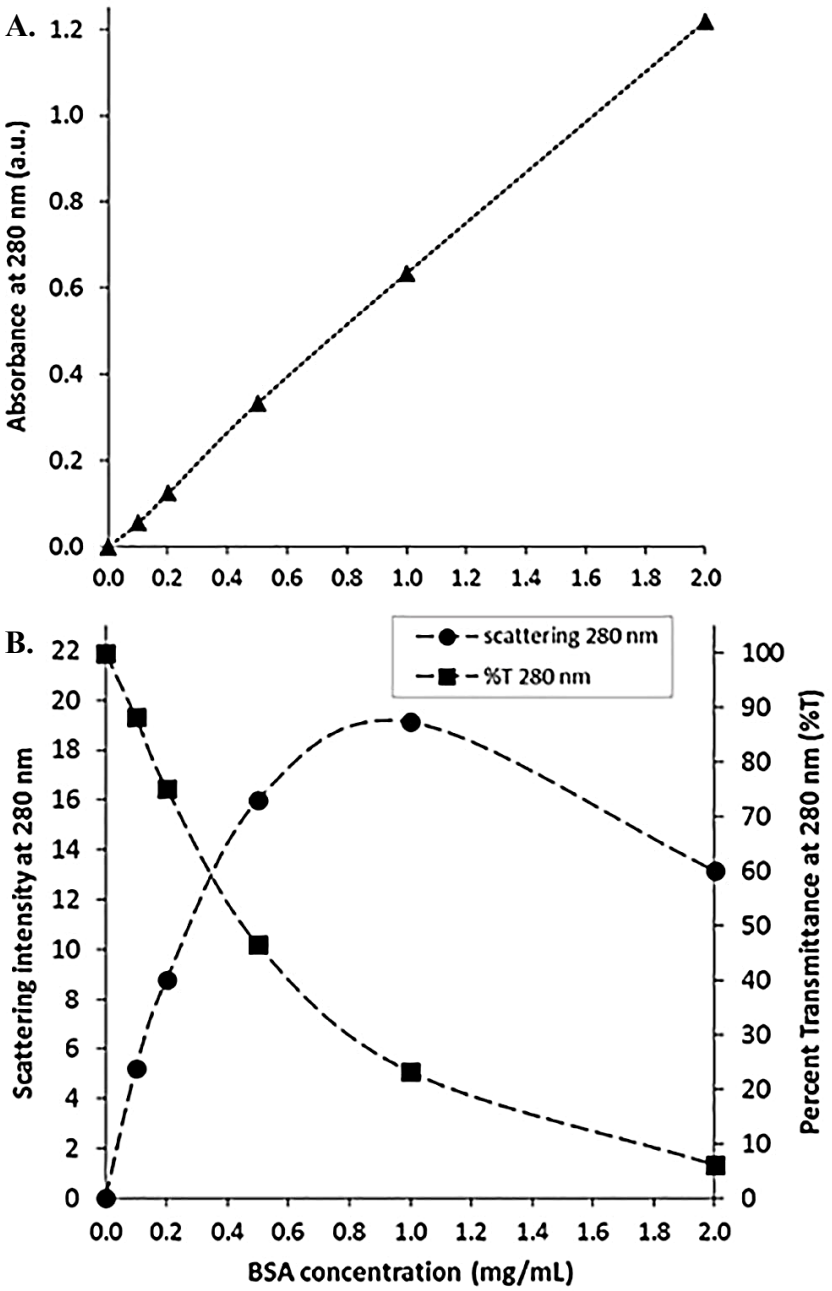

Figure 9. Shows A) absorption intensity and B) scattering intensity and percent transmittance measured at 280 nm as a function of BSA concentration. Absorbance and percent transmittance at 280 nm were measured using a UV spectrometer. Scattering intensities at 280 nm were measured using 90º fluorescence spectrometer. Lines joining the data points are to guide the eye and are not a result of fitting a model to the data.

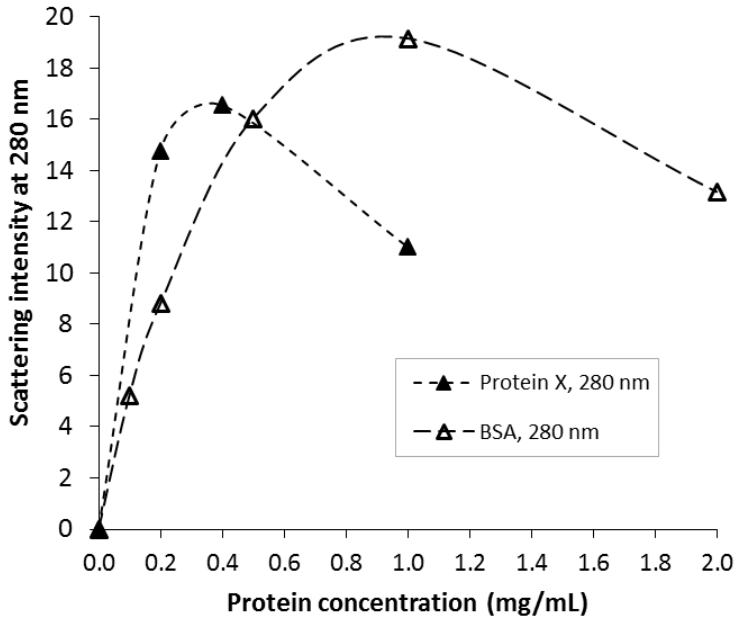

Figure 10. Comparison of scattering intensity at 280 nm for BSA (open triangles) and protein X (solid triangles) as a function of protein concentration. Lines joining the data points are to guide the eye and are not a result of fitting a model to the data.

Chapter 4

UV Light Scattering as a High-Throughput Technique for Detecting Reversible Self-Association in Protein solutions

CONTENTS

Chapter 4

1. ABSTRACT

Reversible self-association in proteins is a concern in pharmaceutical development because of its contribution to product viscosity, irreversible aggregation upon storage and reduced bioavailability. Analytical ultracentrifugation (AUC) is the most commonly used technique for characterizing protein self-association. Although, AUC provides a quantitative analysis of self-association, it is seldom used in early product development. The objective of this work is to investigate the application of ultraviolet light scattering as a high-throughput technique to detect self-association in protein formulations. β-lactoglobulin A and glutamate dehydrogenase were used as model protein systems for the studies. Rayleigh light scattering intensities at 280 and 350 nm were measured using a fluorescence spectrometer at 90º scattering angle. The studies demonstrates that UV light scattering can be used as a rapid, high-throughput technique for detecting self-association in proteins at an early development.

KEYWORDS: protein self-association, UV light scattering, Rayleigh scattering, protein absorption, high-throughput screening

2. INTRODUCTION

Monoclonal antibodies (MAb) and their derivatives have emerged as one the most promising class of biological therapeutics in the past few decades.[1,2] Reversible self-association and aggregation are two of the major challenges associated with formulating high concentration protein therapeutics.[3,4] The term self-association is used for the reversible, non-covalently bonded protein aggregates. Reversible aggregates can significantly increase solution viscosity affecting manufacturing and delivery.[3,5,6] Self-associated proteins can also affect bioavailability and pharmacokinetic properties.[7] Additionally, the long term storage of self-associated molecules can generate covalent linkages resulting in formation of irreversible aggregates.[8-10]

Analytical ultracentrifugation (AUC) is the most commonly used technique for quantitatively studying self-association in proteins.[11] Although it is one of the most reliable tools available for characterizing self-association, it is seldom used in early product development because of the long experiment times, inability to perform high-throughput analysis, higher level of operator expertize and complex data analysis. Several high pressure liquid chromatography (HPLC) based techniques have also been used to characterize protein self-association including self-interaction chromatography (SIC)[12] and size-exclusion chromatography (SEC).[13] Although these techniques are quantitative methods to study stoichiometry and extent of self-association, there are limitations associated with these techniques. For example, SIC requires immobilization of proteins to the column particles. The immobilization of proteins can lead to structural changes which can give erroneous results.[14] SEC requires simultaneous measurements of concentration and scattering intensity to characterize protein self-association.[13] This method has potential for use in high-throughput screening of lead candidates, however, a major drawback is that the sample gets diluted during

SEC analysis. Consequently, the information about the concentration based protein self-association goes undetected.

A number of studies have been reported to understand the mechanism of self-association in proteins. From the literature two model proteins were selected, β-lactoglobulin A (β-lg A) and bovine liver glutamate dehydrogenase (GDH). β-lg A has been characterized extensively for its self-association behavior under acidic conditions. At pH 3, i.e. two units away from the pI (5.2)[15] of β-lg A, protein molecules carry a net positive charge. Thereby, β-lg A exists majorly as a monomer due to electrostatic repulsions between the charged residues. However, upon addition of salt, the charges are screened and the equilibrium is shifted towards the dimer formation. Dimerization takes place because salts screen the electrostatic charge repulsion by anion binding to the positively charged residues and the intrinsic hydrophobic attractions form β-lg A dimers. It is reported that in the presence of greater than 1.0 M salt at pH 3.0, β-lg A exists majorly as a dimer.[13,16] GDH on the other hand has a concentration based oligomerization at pH 7 in the presence of 0.2 M sodium phosphate and 10^{-3} M EDTA.[17] Change in solution pH, ionic strength and protein concentration have been reported as causes of reversible protein self-association making β-lg A and GDH great model systems for our studies.[5,6,10,18]

The main focus of this work is to develop UV light scattering as a technique to detect self-association in protein solutions by using β-lg A and GDH as the model proteins. This is a rapid technique to detect self-association in proteins under different formulation conditions. It does not involve extensive mathematical analysis or dilution of samples thus, providing a fast method for screening lead candidates in early product development.

3. EXPERIMENTAL SECTION

3.1.Materials

All chemicals and buffer reagents used were of highest purity and were purchased from commercial sources. β -lactoglobulin A and bovine liver glutamate dehydrogenase (type I crystalline suspension in ammonium sulfate) were obtained from Sigma-Aldrich (St. Louis, Missouri) and used without further purification. The different properties of the proteins used are listed in table 1. The buffer reagents obtained from Fisher Scientific (Fair Lawn, NJ, USA) were as follows: glycine-HCl for pH 2.3 and 3.0; monobasic-dibasic sodium phosphate for pH 7.0; and 0.5 M EDTA.

3.2.Methods

3.2.1.Sample Preparation

Buffers were prepared at the required ionic strength by dissolving the desired buffer salts in triple distilled water. The buffer pHs (if needed) were adjusted using 1 N HCl or NaOH and filtered using a 0.1 μm filter (Milipore, MA, USA). The protein stocks were prepared by multiple buffer exchange cycles in the desired buffer. Allegra X-15R centrifuge (Beckman Coulter, Indianapolis, IN) and Amicon Ultra centrifugation dialysis tubes (Millipore, Billerica, MA), with 10 kDa MWCO were used for buffer exchange. Four to six buffer exchange cycles were performed at 3000 rcf and 10 °C. At the end of dialysis, the pH of the protein stock was checked to ensure it was within $\pm$ 0.05 of the target value. Two β-lg A stocks were prepared one at pH 2.3 using 20 mM glycine-HCl buffer (No NaCl) and the other at pH 3.0 using similar buffer with 1 M NaCl. β-lg A samples of 2, 4, 6, 8 and 10 mg/mL were made by serial dilution of stock in pH 2.3 and 3.0 buffers. GDH stock of ~10 mg/mL was prepared in 200 mM sodium phosphate

and 10^{-3} M EDTA, pH 7 buffer. GDH samples of 0.04, 0.1, 0.5, 1, 2, 3, 4, 5 and 6.2 mg/mL were prepared. The protein stock concentrations were measured at 280 nm using variable pathlength spectrometer, Solo VPE (C Technologies Inc., Bridgewater, NJ) and performing buffer correction.

3.2.2. Light Scattering Studies

Light scattering intensities were measured at a 90° angle to the incident light source using Photon Technology International (PTI) spectrofluorometer. PTI has a xenon arc lamp as a light source with a wavelength range of 200 – 1100 nm. LS intensities were measured by setting the excitation and emission monochromators both set to the same wavelength. These light scattering intensity scans are also referred to as synchronous scans. A scan rate of 1 nm/sec and average of 3 scans per sample were used. The two wavelengths used for these studies were 280 and 350 nm. A three window and 50 µL sample volume quartz cuvette was used for all the measurements at room temperature.

4. RESULTS

4.1. NaCl dependent dimerization of β-lactoglobulin A, β-lg A (M.W. 18.36 kDa)

The scattering intensities of β-lg A samples were measured at pH 2.3 (no NaCl) and pH 3.0 (1.0 M NaCl). Figure 1A shows the change in scattering intensity at 280 nm as a function of β-lg A concentration under both solution conditions that were tested. At each β-lg A concentration the scattering intensity in pH 2.3 (no NaCl) buffer was less than that of pH 3.0 (1 M NaCl) buffer,

for example, the scattering intensity of 2 mg/mL β-lg A was 19716 at pH 2.3 and 50828 at pH 3.0 (1 M NaCl) buffer.

Fig 1B represents the change in scattering intensity of β-lg A samples measured at 350 nm as a function of protein concentration. The light scattering intensity increased linearly as a function of β-lg A concentration in both pH 2.3 and 3.0 buffers. The scattering intensities for β-lg A were higher at pH 3.0 compared to pH 2.3 at each concentration. For example, the scattering intensity of 2 mg/mL β-lg A was 93,405 in pH 2.3 and 229,088 in pH 3.0 (1 M NaCl) buffer.

4.2. Concentration dependent oligomerization of bovine liver glutamate dehydrogenase, GDH (M.W. 318 kDa)

The oligomerization of bovine liver GDH was investigated in pH 7.0 buffer containing 0.2 M sodium phosphate and $1.0X10^{-3}$ M EDTA. Figure 2 shows the change in scattering intensity as a function of GDH concentration. Figure 2A shows the scattering intensity change measured at 280 nm where, GDH has an attenuation coefficient (formerly called extinction coefficient[19]) of 0.973 mL/mg.cm. The scattering intensity increased with an increase in GDH concentration until 2 mg/mL. At concentrations greater than 2 mg/mL the scattering intensity decreased as a function of GDH concentration.

Figure 2B shows the change in the scattering intensity for GDH as a function of concentration at 350 nm incident wavelength. The scattering intensities increased linearly with concentration up to 1 mg/mL. A non-linear increase in scattering intensities was observed at concentrations greater than 1 mg/mL.

5. DISCUSSION

5.1. NaCl dependent dimerization of β-lactoglobulin A

β-lactoglobulin A (β-lg A) dimerizes in the presence of salt under acidic conditions. The association constant for dimerization of β-lg A depends on the concentration of the salt present in the solution.[13,16] β-lg A exists primarily as a monomer in pH 2.3 glycine-HCl buffer in the absence of additional salts. At pH 3.0 a reversible monomer-dimer equilibrium exists in the presence of NaCl. The self-association constant for β-lg A depends on the concentration of NaCl in the solution. β-lg A exists primarily as a dimer in the presence of 1 M NaCl at pH 3.0.[13] β-lg A has a monomer-dimer type of reversible reaction as a function of NaCl concentration around pH 3.0 given by the following reaction scheme:

$$M + M \rightleftharpoons D$$

where M and D represent β-lg A monomer and dimer, respectively. The scattering intensities of β-lg A samples were measured at two solution conditions. In pH 2.3 glycine HCl buffer (without any additional salts) the equilibrium shifts to the left and β-lg A predominantly exists as a monomer. In pH 3.0 glycine HCl buffer (presence of 1 M NaCl), the equilibrium shifts to the right and β-lg A exists primarily as a dimer. Sodium chloride shields the charges by binding the anion with the positively charged protein residues. This decreases the electrostatic repulsions and promotes dimer formation due to intrinsic hydrophobic attractions.[16]

Figure 1A shows a decrease in scattering intensity as a function of β-lg A concentration at at 280 nm. For an ideal system light scattering varies linearly with protein size and concentration. However, at 280 nm, scattered intensity is also affected by the extent of reabsorption by protein chromophores. Therefore, scattering intensity decreases as a function of

β-lg A concentration. The intensity of scattered light measured at 280 nm is given by the following equation (refer chapter 3):

$$i_s(measured) = K(1 + cos^2\theta)I_0 cM * 10^{-a_{abs}cl} \qquad \textit{Equation 1}$$

where θ is the scattering angle, I_0 is the initial intensity of light source, l is the optical pathlength, c, M and a_{abs} are concentration, molecular weight and attenuation coefficient of the scattering molecule, respectively and

$$K = \frac{8\pi^2 n_0^2}{N_A \lambda_0^2}\left(\frac{dn}{dc}\right)^2$$

The optical constant K depends on the solution refractive index (n_0), Avogadro's number (N_A), wavelength of incident light (λ_0) and change in refractive index of the scattering molecule (dn/dc). Rearranging and taking a log of equation 1 gives:

$$\log\frac{i_s}{c} = \log\{K(1 + cos^2\theta)I_0 M\} - (a_{abs}cl) \qquad \textit{Equation 2}$$

The scattering due to solute is calculated by subtracting the buffer contribution. At non absorbing wavelengths the buffer contribution is measured in the absence of the solute and subtracted from the sample readings. However, at absorbing wavelengths the buffer scattering contribution decreases with increase in solute (i.e. protein) concentration due to reabsorption by protein chromophores. The buffer scattering contribution ($i'_{s,c}$) is a function of β-lg A concentration (c) and is given by the following equation (refer chapter 3):

$$i'_{s,c} = i'_{s,0}10^{-a_{abs}cl} \qquad \textit{Equation 3}$$

where $i'_{s,0}$ is the scattering intensity of buffer in the absence β-lg A. The buffer contribution was calculated at each β-lg A concentration and subtracted from the sample reading to obtain scattering due to β-lg A only, as shown in table 2.

At non absorbing wavelengths, the scattering intensity is a function of optical constant (K), scattering angle (θ), intensity of unpolarized light source (I_0), concentration (c) and average molecular weight (M) of the scattering species given by the following equation:

$$i_s = K(1 + cos^2\theta)I_0cM \qquad \textit{Equation 4}$$

The scattering intensity at 350 nm increased as a function of β-lg A concentration as shown in figure 1B. The increase was linear in both monomeric and dimeric β-lg A samples. At each β-lg A concentration the increase in scattering intensity was higher at pH 3.0 (1 M NaCl) compared to pH 2.3. This is because the scattering intensity is directly proportional to the molecular weight of the scattering molecule and molecular weight of β-lg A in pH 3.0 is two times of that in pH 2.3. The lines in the figure represent linear fits to the data using the following equations:

pH 2.3 glycine HCl buffer with 0 M NaCl: $y = 36456x + 14159$ *Equation 5*

pH 3.0 glycine HCl buffer with 1 M NaCl: $y = 106161x + 18404$ *Equation 6*

The slopes of the equations obtained by linear fit provide information about the molecular weight of β-lg A in pH 2.3 and 3.0 glycine HCl buffers. Ratio of the slopes was taken to obtain the degree of oligomerization, (Slope2)/(Slope1) = 106161/36456 = 2.91.

The degree of oligomerization shows a deviation from 2 (value for dimerization) because the value of dn/dc is different for pH 2.3 (0 M NaCl) and pH 3.0 (1 M NaCl) that was not accounted, while taking the ratio of either intercepts or slopes. The value of dn/dc is unknown

in the UV range because the current techniques used to measure dn/dc are limited to higher wavelengths (>500 nm). However, corrections were made using the factor R, given by:

$$R = \frac{(dn/dc)^2_{pH3.0,\ 1M\ NaCl}}{(dn/dc)^2_{pH2.3,\ 0M\ NaCl}} = \frac{(0.145)^2}{(0.162)^2} = 0.801$$

The correction factor R was calculated using the dn/dc values reported in literature at 685 nm (Bajaj 2007). The degrees of oligomerization obtained after multiplying with the correction factor were as follows:

a) At 280 nm is $2.80 * 0.801 = 2.24$

b) At 350 nm is $2.91 * 0.801 = 2.33$

Appropriate corrections should lead to more accurate calculation of the degree of oligomerization. Further studies need to be performed to determine the refractive index increment used to calculate the correction factor R for proteins in the UV range. However, these studies demonstrate the potential of UV light scattering as a fast and efficient tool for screening proteins under different solution conditions to prevent manufacturing and formulation challenges due to self-association.

5.2. Concentration dependent oligomerization in bovine liver glutamate dehydrogenase

It is widely reported in literature that GDH undergoes a concentration based reversible oligomerization in pH 7 buffer. The molecular weight of a monomer of GDH was reported to be 53.5 kDa.[17,20] However, at pH 7 in the presence of 0.2 M sodium phosphate and 10^{-3} M EDTA, GDH forms hexamers of the molecular weight 318 kDa calculated at infinite dilution using

multiple angle static light scattering.[17] It was also found that the molecular weight of GDH increased infinitely with concentration up to 8 mg/mL at this solution condition.[17] With an increasing GDH concentrations the hexamers self-associate to form higher molecular weight species given by the following reaction scheme:

$$6\,M \rightarrow H \rightleftharpoons Z$$

where M, H and Z represent GDH monomer, hexamer and higher order reversible aggregates, respectively. Therefore, GDH serves as a good model protein to assess the applicability of UV light scattering to detect concentration based self-association.

The light scattering intensity at 280 nm first increased and then decreased as a function of GDH concentration giving a scatter maximum around 2 mg/mL as shown in figure 2A. As mentioned in section 4.1, the scattering intensity of proteins at 280 nm is a function of the concentration, molecular weight of the protein and the secondary absorption due to chromophores. The scattering intensity increases with increase in concentration and molecular weight of GDH, whereas it decreases due to a fraction reabsorbed by the chromophoric groups. The measured scattering intensity is the sum of these two opposite effects. For GDH the scatter intensity increased up to 2 mg/mL as a function of GDH concentration. The increase in reabsorption at concentrations higher than 2 mg/mL decreased scattering intensity. The position of scatter maximum depends on the molecular weight and molar absorbance of the protein. Unlike β-lg A, the scattering intensity of GDH (plotted on a log scale) does not decrease linearly as a function of GDH concentration (shown in figure 4). It has been reported in literature that GDH self-associates as a function of concentration resulting in a change of molecular weight.[17] The non-linear dependence of plots in figure 4 indicates the presence of self-association in GDH

samples but, a detailed mathematical understanding is required to calculate the average molecular weight of GDH at each concentration using this data.

At 350 nm the light scattering intensities increased with an increase in GDH concentration as shown in figure 2B. Unlike β-lg A, the light scattering intensity increased non-linearly as a function of GDH concentration. The increase was non-linear due to a concentration based increase in the molecular weight of GDH in the solution. The change in scattering intensity qualitatively correlates with the change in molecular weight of GDH as a function of concentration. The molecular weight of GDH increased by 3 folds when concentration was increased from 0.1 to 2 mg/mL as reported by Eisenberg et al.[17] Accordingly, the light scattering intensity measured at 350 nm increased by 36 times for the same concentration change. The magnitude of change in scattering intensities was greater at concentrations less than 1 mg/mL. At concentration of 2 mg/mL or greater the magnitude of scattering intensity increase was smaller.

6. SUMMARY AND CONCLUSIONS

UV light scattering intensities are sensitive to the presence of protein oligomers. The scattering intensity at 350 nm increased as a function of protein concentration for both β-lg A and GDH. When a single species (monomer or dimer) was majorly present, the scattering intensity was directly proportional to protein concentration, as seen in the case of β-lg A and the slope can be related to the molecular weight of the species. However, when more than one type of species were present (i.e. a mix of monomer, dimer or other oligomers), a non-linear increase in scattering intensity was observed as seen in the case of GDH. The studies demonstrates that

UV light scattering can be used as a fast and rapid tool for detecting self-association in proteins. It can be used to screen proteins under different solution pH and ionic strength.

7. REFERENCES

1. Aggarwal, S. R. What's fueling the biotech engine-2012 to 2013. *Nat. Biotechnol.* **2014***, 32*, 32-39.
2. Carlson, R. Estimating the biotech sector's contribution to the US economy. *Nat Biotech* **2016***, 34*, 247-255.
3. Shire, S. J. Formulation and manufacturability of biologics. *Curr. Opin. Biotechnol.* **2009***, 20*, 708-714.
4. Wang, W. Protein aggregation and its inhibition in biopharmaceutics. *Int. J. Pharm.* **2005***, 289*, 1-30.
5. Liu, J.; Nguyen, M. D. H.; Andya, J. D.; Shire, S. J. Reversible self-association increases the viscosity of a concentrated monoclonal antibody in aqueous solution. *J. Pharm. Sci.* **2005***, 94*, 1928-1940.
6. Kanai, S.; Liu, J.; Patapoff, T. W.; Shire, S. J. Reversible self-association of a concentrated monoclonal antibody solution mediated by fab-fab interaction that impacts solution viscosity. *J. Pharm. Sci.* **2008***, 97*, 4219-4227.
7. Brems, D. N.; Alter, L. A.; Beckage, M. J.; Chance, R. E.; Dimarchi, R. D.; Green, L. K.; Long, H. B.; Pekar, A. H.; Shields, J. E.; Frank, B. H. Altering the association properties of insulin by amino acid replacement. *Protein Eng. Des. Sel.* **1992***, 5*, 527-533.
8. Cromwell, M. E. M.; Hilario, E.; Jacobson, F. Protein aggregation and bioprocessing. *AAPS Journal* **2006***, 8,* E572-E579.
9. Philo, J. S. Is any measurement method optimal for all aggregate sizes and types? *The AAPS Journal* **2006***, 8*, E564-E571.
10. Saluja, A.; Kalonia, D. S. Nature and consequences of protein-protein interactions in high protein concentration solutions. *Int. J. Pharm.* **2008***, 358*, 1-15.
11. Howlett, G. J.; Minton, A. P.; Rivas, G. Analytical ultracentrifugation for the study of protein association and assembly. *Curr. Opin. Chem. Biol.* **2006***, 10*, 430-436.
12. Le Brun, V.; Friess, W.; Bassarab, S.; Mühlau, S.; Garidel, P. A critical evaluation of self-interaction chromatography as a predictive tool for the assessment of protein–protein interactions in protein formulation development: A case study of a therapeutic monoclonal antibody. *European Journal of Pharmaceutics and Biopharmaceutics* **2010***, 75*, 16-25.
13. Bajaj, H.; Sharma, V. K.; Kalonia, D. S. A high-throughput method for detection of protein self-association and second virial coefficient using size-exclusion chromatography through simultaneous measurement of concentration and scattered light intensity. *Pharm. Res.* **2007***, 24*, 2071-2083.
14. Tessier, P. M.; Lenhoff, A. M. Measurements of protein self-association as a guide to crystallization. *Curr. Opin. Biotechnol.* **2003***, 14*, 512-516.
15. Zimet, P.; Livney, Y. D. Beta-lactoglobulin and its nanocomplexes with pectin as vehicles for ω-3 polyunsaturated fatty acids. *Food Hydrocolloids* **2009***, 23*, 1120-1126.

16. Sakurai, K.; Oobatake, M.; Goto, Y. Salt-dependent monomer-dimer equilibrium of bovine ß-lactoglobulin at pH 3. *Protein Sci.* **2001***, 10*, 2325-2335.
17. Eisenberg, H.; Tomkins, G. M. Molecular weight of the subunits, oligomeric and associated forms of bovine liver glutamate dehydrogenase. *J. Mol. Biol.* **1968***, 31*, 37-49.
18. Shire, S. J.; Shahrokh, Z.; Liu, J. Challenges in the development of high protein concentration formulations. *J. Pharm. Sci.* **2004***, 93*, 1390-1402.
19. IUPAC. Compendium of Chemical Terminology, 2nd ed. (the "Gold Book"). Compiled by A. D. McNaught and A. Wilkinson. Blackwell Scientific Publications, Oxford (1997). XML on-line corrected version: http://goldbook.iupac.org (**2006**-) created by M. Nic, J. Jirat, B. Kosata; updates compiled by A. Jenkins. ISBN 0-9678550-9-8. https://doi.org/10.1351/goldbook. .
20. Eisenberg, H.; Reisler, E. A physical model for the structure of glutamate dehydrogenase. *Biopolymers* **1970***, 9*, 113-115.
21. Pace, C. N.; Vajdos, F.; Fee, L.; Grimsley, G.; Gray, T. How to measure and predict the molar absorption coefficient of a protein. *Protein Science* **1995**, *4*, 2411-2423.

8. TABLES

Table 1. Properties of the model proteins used for the studies

Protein	Abbreviation	λ (nm), $\varepsilon^{1\%}$ (cm^{-1})	MW (kDa)
β-lactoglobulin A	β-lg A	280, 9.60[a]	18.36[a]
Glutamate dehydrogenase, bovine liver	GDH	279, 9.73[b]	53.00[b]

a. *Pace et al. 1995,[21] b. Eisenberg et al. 1968.[17]*

Table 2. Correction of scattering intensity of β-lg A for buffer contribution at 280 nm.

β-lg A Concentration (mg/mL)	Buffer contribution	β-lg A scatter intensity (Sample)	Excess scatter = sample – buffer
β-lg A in pH 2.3 glycine buffer			
0	92027.0	92027.0	0.0
2	24429.5	44145.3	19715.7
4	6485.1	19586.0	13100.9
6	1721.5	8152.4	6430.9
8	457.0	4262.8	3805.8
10	121.3	3380.5	3259.2
β-lg A in pH 3.0 glycine buffer + 1.0 M NaCl			
0	95846.8	95846.8	0.0
2	25443.6	76271.8	50828.2
4	6754.3	36524.4	29770.1
6	1793.0	15647.7	13854.7
8	476.0	7795.7	7319.7
10	126.4	4384.4	4258.0

9. FIGURES

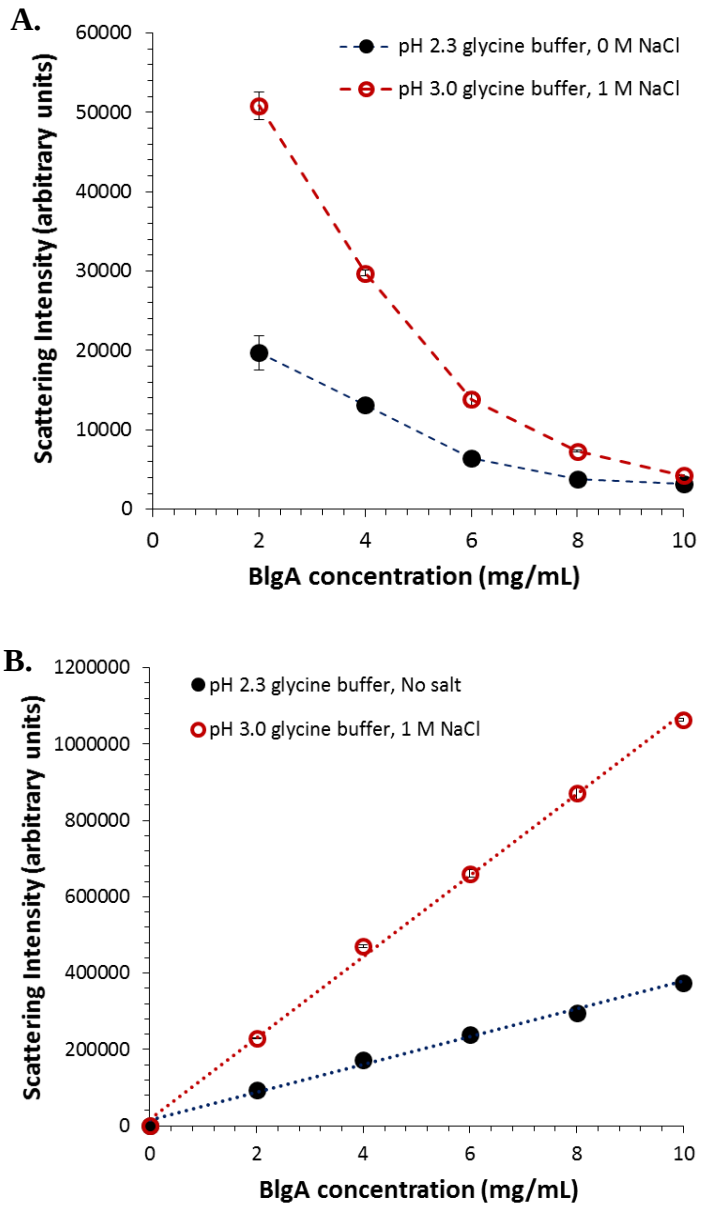

Figure 1. Scattering intensity as a function of β-lg A concentration measured at A) 280 nm and B) 350 nm. The closed and open symbols represent respectively the scattering intensity of β-lg A samples in pH 2.3 glycine-HCl buffer (0 M NaCl) and pH 3.0 glycine-HCl buffer (1 M NaCl). The lines joining the symbols in figure 1A are to guide the eye and are not data points. The lines joining the data points in figure 1B are obtained by performing liner fit to the data.

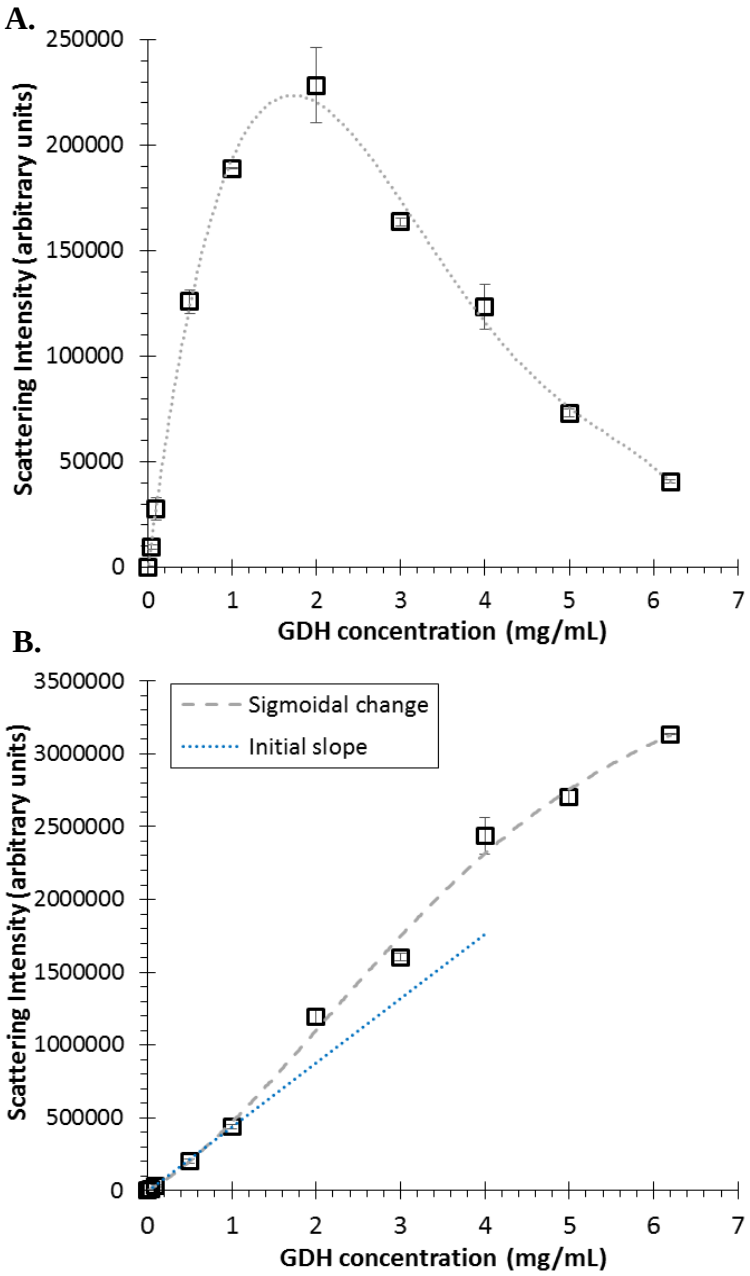

Figure 2. Scattering intensity as a function of GDH concentration measured at A) 280 nm and B) 350 nm. The lines joining the data points are obtained by performing polynomial fit to the data.

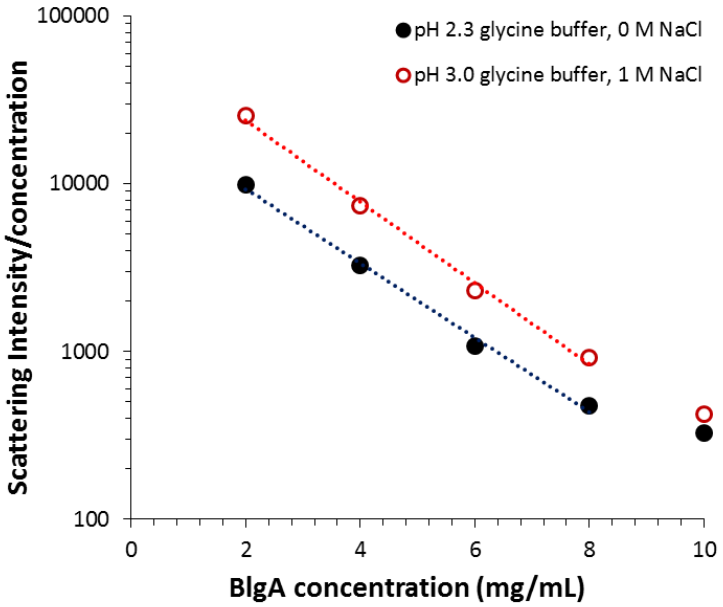

Figure 3. Log of the ratio of scattering intensity at 280 nm and β-lg A concentration as a function of β-lg A concentration. The closed and open symbols represent respectively, the measurements of β-lg A samples in pH 2.3 glycine buffer (0 M NaCl) and pH 3.0 glycine buffer (1 M NaCl). The lines joining the data points are obtained by performing exponential fit to the data.

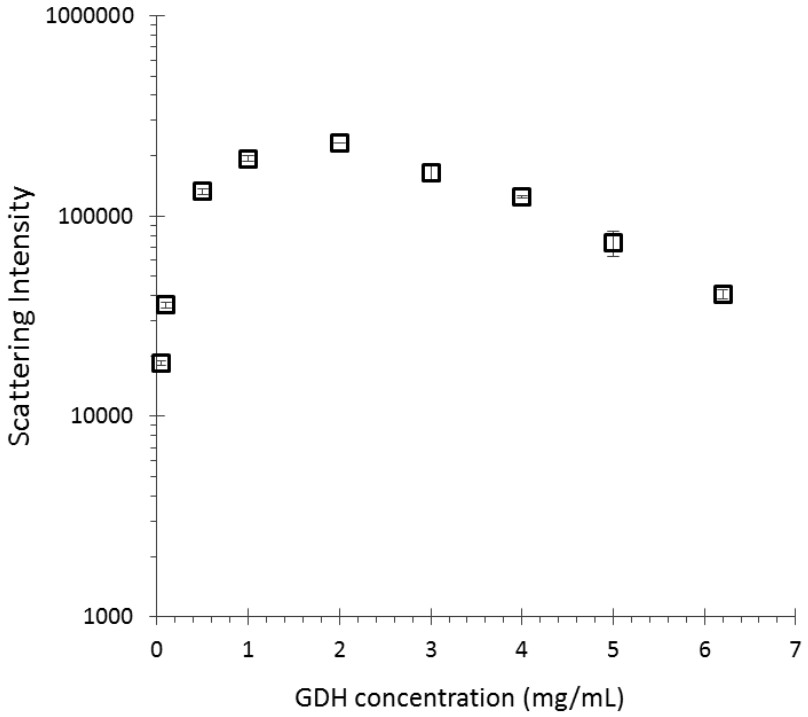

Figure 4. Scattering intensity (on a log scale) as a function of GDH concentration measured at 280 nm.

Chapter 5

Application of Ultraviolet light scattering to detect protein aggregation in solution

CONTENTS

Chapter 5

1. ABSTRACT

The objective of this work is to investigate the application of UV light scattering as a technique to detect changes in aggregate content in a 2 – 50 mg/mL protein concentration range. Aggregation is a major degradation pathway of protein-based therapeutics, making it an important concern when developing formulations. Size exclusion high pressure liquid chromatography (SE-HPLC) is the most commonly used technique for measuring the aggregate content in protein solutions. The major drawback of SE-HPLC is that it requires sample dilution prior to analysis which can result in loss of information about reversible aggregates. The proteins used in the study were bovine serum albumin (BSA), β-lactoglobulin (β-lg) and protein X. Aggregation was induced in the protein systems by heating the samples at elevated temperatures. Change in light scattering intensities (at 350 nm) on heating was compared to aggregate content measured using SE-HPLC. The studies demonstrate that UV light scattering can be used as a rapid tool for detecting the change in concentration of aggregates and approximately estimate the molecular weights of the higher order aggregates present in the protein solutions. The major advantage of this technique is that the protein samples can be analyzed at the same concentrations at which they are formulated i.e. it eliminates the need to dilute the samples before analysis providing a more representative analysis of aggregation.

2. **KEY WORDS:** protein aggregation, UV light scattering, Rayleigh scattering, high concentration

3. INTRODUCTION

Aggregation is one of the major degradation pathways affecting the physical stability of proteins.[1] Aggregation can occur at different stages of the production cycle of proteins i.e. purification, processing, formulation and storage.[2] Protein aggregates can cause immunogenic reactions, decrease potency of drug and increase solution viscosity thereby, negatively affect manufacturing, delivery and quality of the protein formulations, making it an important concern when developing formulations.[1,3,4]

Aggregation can be due to reversible or irreversible association of proteins.[5,6] Reversible aggregation (also called self-association) depends on the equilibrium between non-associated and higher order forms of native proteins.[7,8] Irreversible aggregation however, can be classified as native or non-native association of proteins. Native-like aggregates are formed by covalent linkages (such as disulfide bonds) between protein species in which the monomer structure remains relatively intact. Non-native aggregates are formed when proteins unfold, exposing the hydrophobic residues and come together to form non-covalently bonded higher order aggregates.[9,10]

Size exclusion chromatography (SEC) is the most commonly used technique to quantitate the aggregate content present in the protein solutions. The major drawback of SEC is that it requires sample dilution and the information about reversible aggregates goes undetected. Several literature studies report that the dilute solution properties are not true representatives of high concentration protein behavior.[11,12] Therefore, there is a need for a technique that can measure protein aggregates in a wide range of concentrations.

It was demonstrated in the previous work (Chapter 4) that UV light scattering is sensitive to the changes in molecular weight of proteins under dilute conditions. The main focus of this work is to investigate the sensitivity of UV light scattering to detect change in aggregate content in protein solutions at a wide range of concentrations. The work is further extended to quantitate the aggregate content and estimate the molecular weight of the higher order species generated on heating the protein samples.

4. EXPERIMENTAL SECTION

4.1. Materials

All chemicals and buffer reagents used were of highest purity and were purchased from commercial sources. B-lactoglobulin (mixture of A & B) and bovine serum albumin (BSA) were obtained from Sigma-Aldrich (St. Louis, Missouri). Protein X, a monoclonal antibody of molecular weight 149 kDa was used. The different properties of the proteins used are listed in table 1. The buffer reagents obtained from Fisher Scientific (Fair Lawn, NJ, USA) were as follows: monobasic-dibasic sodium phosphate for pH 7.0.

4.2.Methods

4.2.1. Sample Preparation

Buffers were prepared at the required ionic strength by dissolving the desired buffer salts in triple distilled water. The buffer pHs (if needed) were adjusted using 1 N HCl or NaOH and filtered using a 0.1 μm filter (Milipore, MA, USA). The protein stocks were prepared by multiple buffer exchange cycles in the desired buffer. β-lg stock was prepared in pH 7, 15 mM sodium

phosphate buffer and samples of 20 and 50 mg/mL were prepared by serial dilution. BSA stock solution of ~200 mg/mL was prepared by dissolving the required amount in pH 7, 15 mM phosphate buffer and samples of 2, 5, 20 and 50 mg/mL were prepared. Similarly, protein X stock was prepared in pH 7, 15 mM sodium phosphate buffer and diluted to 2, 5, 20 and 50 mg/mL. The protein stock concentrations were measured at 280 nm using variable pathlength spectrometer, Solo VPE (C Technologies Inc., NJ) and performing buffer correction.

4.2.2. Light Scattering Studies

Light scattering intensities were measured at a 90° angle using Photon Technology International (PTI) spectrofluorometer. The measurements were performed by setting the excitation and emission monochromators both set to the same wavelength. The studies were done at the wavelength of 350 nm. A three window and 50 μL sample volume quartz cuvette was used for all the measurements at room temperature.

4.2.3. Selection of heating temperature for proteins

The thermal unfolding profiles of the proteins were used to select the heating temperatures for accelerating aggregation. Literature reported Thermal unfolding profiles were used for BSA and β-lg samples.[13,14] BSA samples of 2, 5, 20 and 50 mg/mL were heated at 58 ºC. β-lg samples of 20 and 50 mg/mL were heated at 65 ºC. Thermal unfolding scan was obtained using differential scanning calorimetry (DSC) to determine the heating temperature for protein X (discussed in section 4.3.1.).

4.2.4. Differential Scanning Calorimetry (DSC)

A nano-DSC (TA Instruments, New Castle, DE) was used to determine onset temperature of unfolding Protein X in 15 mM phosphate buffer at pH 7. The reading for blank solutions was

measured with buffer in both the sample and reference cell before the measurement of the actual samples. 1 mg/ml of BSA and Protein X were analyzed at a scan rate of 1°C/min from 25°C–95°C. The scans were baseline subtracted and analyzed using the NanoAnalyze software (TA Instruments).

4.2.5. Heating of protein solutions

BSA, β-lg and Protein X samples were heated respectively at 58, 65 and 63 ºC by using the Isotemp incubator (Fisher Scientific). All the samples were filtered using a 0.22 μm syringe filter before heating. The heating temperatures were selected based on the thermal unfolding profiles of the respective proteins obtained using nano-DSC (TA Instruments, New Castle, DE), whereas, sampling time points were selected depending upon protein concentrations. The aggregates were measured at time points: 0, 1 and 3 hours for all concentrations of BSA; 0, 3, 5 and 6 hours for 20 mg/mL β-lg; 0, 1, 2 and 3 hours for 50 mg/mL β-lg; 0, 5, 7 and 12 hours for 2 and 5 mg/mL protein X; 0, 1, 2 and 3 hours for 20 and 50 mg/mL protein X.

4.2.6. Size-exclusion high performance liquid chromatography (SE-HPLC)

Soluble monomer and aggregate content was analyzed using SE-HPLC with an inline UV detector set at a wavelength of 280 nm. 100 mM sodium phosphate buffer (pH 7.0) at a total ionic strength of 200 mM (ionic strength adjusted with NaCl) was used as the mobile phase. A 300 x 7.8 mm TSK G3000 SW XL gel filtration column (Tosoh Biosciences, LLC) was used at an isocratic flow rate of 1 ml/min with an injection volume of 40 mL. All the samples were diluted to 2 mg/mL protein concentration in phosphate buffer (pH 7.0 and ionic strength 15 mM) and filtered using 0.22 μm syringe filter prior to injection. Peak Simple 3.88 (SRI Instruments,

Torrance, CA) software was used to analyze the area under the peak for the chromatograms. The chromatograms collected for samples before heating were labeled as T=0.

5. RESULTS

5.1. Heat Induced Aggregation of Bovine Serum Albumin (BSA) Samples

Figure 1 compares the change in percent aggregates and light scattering intensities for 2, 5, 20 and 50 mg/mL BSA samples before and after heating at 58 ºC. The x-axis represents specific concentrations of proteins. The results show that all BSA samples contained 28.5% aggregates before heating (T = 0), represented by the solid black line. The extent of aggregation increased with time of exposure to 58 ºC at each concentration. The Rayleigh light scattering (secondary y-axis) represented by symbols was measured at 350 nm without subjecting the sample to any additional processing step (e.g. filtration or dilution). Light scattering intensities also increased when the BSA samples were heated. The increase in scattering intensities was higher at higher concentrations and longer heating times.

5.2. Heat Induced Aggregation of β-lactoglobulin (β-lg) Samples

Figure 2 shows the UV chromatograms (280 nm) for β-lg solutions before (T = 0) and after heating 20 mg/mL samples at 65 ºC for 3, 5 and 6 hours. The chromatograms show a significant decrease in the monomer peak upon thermal stress. Chromatograms show that the percentage of soluble aggregates increased with the longer heating times. Similar chromatographic profile was observed on heating 50 mg/mL β-lg samples (data not shown) and aggregation occurred at a faster rate for 50 versus 20 mg/mL β-lg samples.

Figures 3 and 4 show the increase in percent aggregates (and thereby an increase in scattering intensity) for 20 and 50 mg/mL β-lg, respectively. 20 mg/mL β-lg samples were heated at 65 ºC for 3, 5 and 6 hours. Whereas, 50 mg/mL β-lg samples were heated at the same temperature for 1, 2 and 3 hours. The percent aggregates measured prior to heating (at T = 0) were less than 0.2 percent, thus was considered negligible compared to monomers. Thereby, the scattering intensity measured at T = 0 is due to the presence of monomers of β-lg (shown by open circles). For both 20 and 50 mg/mL β-lg, percent aggregate content and scattering intensity increased when samples were heated for longer time periods. More than 40% aggregates were formed by heating 50 mg/mL β-lg for 3 hours and 40% aggregates were formed by heating 20 mg/mL β-lg for 6 hours.

5.3. Heat induced aggregation of Protein X

5.3.1. Protein X Unfolding and heating temperatures

DSC scans were performed to determine the temperature of unfolding for protein X as shown in figure 5. The onset temperature of unfolding obtained from the thermal scans was 63 ºC. For dilute samples (2 and 5 mg/mL protein X), the heating studies were performed at 65 ºC i.e. two degrees higher than onset of unfolding temperature to accelerate aggregation. For 20 and 50 mg/mL samples the heating studies were performed at 63 ºC i.e. at the onset of unfolding.

5.3.2. Aggregation studies for dilute protein X solutions

Figure 6 represents the change in percent aggregates (and consequent change in scattering intensities measured at 350 nm) on heating 2 and 5 mg/mL protein X samples at 65 ºC for 0, 1, 2 and 3 hours. The samples contain ~1.2 percent aggregates prior to heating (i.e. at T = 0). The amount of aggregates formed was greater for 5 mg/mL versus 2 mg/mL protein X at each time point, shown by bar graphs. 10 % and 15 % aggregates were formed after heating 2 and 5 mg/mL

respectively, for 3 hours at 65 ºC. The light scattering intensity (secondary y-axis) change after 1 hour of heating was negligible for 2 (triangles) and 5 (circles) mg/mL protein X. However, heating the samples for longer time periods increased the scattering intensity.

5.3.3. Aggregation studies for concentrated protein X solutions

Figure 7 shows the change in percent aggregates measured by SEC and light scattering intensities at 350 nm for 20 and 50 mg/mL protein X samples. The samples were heated at 63 ºC for 0, 1, 2 and 3 hours. For 20 mg/mL protein X, 1% aggregates were present in samples at T = 0 and increased to 8% on heating the samples for 3 hours at 63 ºC. For 50 mg/mL protein X, the percent aggregates increased to 13.4 percent on heating the sample for 3 hrs at 63 ºC. The amount of soluble aggregates formed was greater for 50 versus 20 mg/mL protein X and for longer heating times. The light scattering intensity measured at 350 nm (secondary y- axis) also increased with formation of soluble aggregates. For 20 mg/mL protein X the scattering intensity did not increase significantly after 1 hour of heating. However, scattering intensity of the sample increased by a factor of 1.6 relative to the initial intensity when heated for 3 hours. For 50 mg/mL protein X the scattering intensity increased with a longer heating times. The scattering intensity of sample increased by 2 folds (compared to initial) when heated for 3 hours at 63 ºC.

6. DISCUSSION

6.1. BSA Aggregation

BSA was used for these studies because of its low cost and easy availability. Prior to heating (T = 0) all the BSA samples contained around 28.5% aggregates. Therefore, the scattering intensity at 350 nm (solid circles) has contribution from both 72.5% monomers and 28.5% aggregates. Since the scattering measurements are made without diluting the samples, the increase

in scattering intensities observed at T = 0 is because of an increase in the concentration of BSA. The amount of aggregates increased with the extent of heating at 58 ºC as measured by SEC. The monomer content decreases with the increase in aggregates. Thereby, the change in scattering intensities after 1 (triangles) and 3 (squares) hour of heating is a function of both BSA concentration and monomer-aggregate content. The change in scattering intensity on heating the samples was greater for 20 and 50 mg/mL BSA (high concentration) compared to 2 and 5 mg/mL BSA. This is because at higher concentration, larger amount of aggregates are formed that will contribute to increase in scattering intensity. However, the sensitivity of the assay decreases due to the presence of aggregates at initial time (high baseline) making this batch of BSA a poor model for assessing the potential of UV light scattering to detect increase in aggregates.

6.2. β-lactoglobulin Aggregation

β-lactoglobulin used for the studies, provides a better model because the protein batch contained less than 0.02% aggregates at T = 0 (low baseline). The heat-induced aggregation mechanism of β-lg in pH 7 low ionic strength buffer is reported in detail by Aymard et al.[15] β-lg exists as a dimer at neutral pH and on heating dissociates into reactive monomers with exposed sulfhydryl groups. The reactive monomers associate to form higher order aggregates. When the samples are heated at 65 ºC, two distinct elution peaks and a small shoulder were observed in the chromatogram (figure 2). This signifies the presence of three species i.e. higher order aggregates, dimer and reactive monomers. The intensity of aggregate peak increased with the increase in incubation time indicating the increase in the aggregate content. 50 mg/mL β-lg samples had similar chromatograms however, concentration of aggregates generated was higher compared to 20 mg/mL β-lg.

<u>Analysis of aggregate content</u>

Table 2.I. compares the change in aggregate-dimer content (measured using SEC) and light scattering intensities on incubating 20 mg/mL β-lg at 65 ºC. The amount of aggregates formed increased with longer heating time because of the formation of higher order aggregates. The change in percent aggregates increased the total light scattering intensity because particles of greater size and concentration scatter more light (refer to Rayleigh scattering equation in chapter 3). For example, heating 20 mg/mL β-lg increased the UV light scattering intensity by a factor of 2.4, 5.0 and 6.0 compared to the initial, in the presence of 13, 33 and 40% aggregates. Table 2.II. summarizes the relationship between changes in the concentration of β-lg species (aggregates and dimers) and increase in scattering intensity on heating 20 mg/mL samples. The calculations were performed using the following assumptions:

1) Molecular weight is the only factor effecting the total scattering intensity of the sample.
2) 'a' is the average molecular weight of β-lg species before heating (T =0).
3) The molecular weight of aggregates is 8a. The approximation was based on the elution time of the aggregate peak.
4) Percent aggregates and dimers measured by SEC were used as the concentration of those species in the samples.
5) Total scattering intensities were calculated by adding the contribution by aggregates and dimers.

The values in last column of Tables 2.I. and 2.II. are the change in scattering intensity of β-lg samples after heating for 3, 5 and 6 hours compared to the initial (T = 0). If the aggregation was a two state model of dimer forming a higher order aggregate with 8 dimer subunits then the scattering intensities will be proportional to the increase in molecular weights. But as aggregation gets complex higher order aggregates of different sizes are formed making the molecular weight

estimations complex and difficult. This explains the deviation of calculations performed in table 2.II.

For 50 mg/mL β-lg samples, the amount of aggregates formed increased both with longer heating times and with higher concentration of proteins. For example, on heating 20 mg/mL β-lg for 3 hours generated 12.8% aggregates, whereas, heating 50 mg/mL β-lg at the same temperature for 3 hours generated 44.5% aggregates. This is because at higher concentrations of proteins in solution means greater amount of reactive proteins and the probability of seeing another protein molecule in solution. In case of 50 mg/mL even the presence of 1.68% aggregates (after heating samples for 1 hr) increased the light scattering intensity by 1.1 times. These studies show that the presence of greater than 2% aggregates can be detected using UV light scattering for β-lg type of proteins.

6.3. Protein X Aggregation

Before heating, the samples were analyzed for amount of aggregates present which were found to be 1.3% for 2 and 5 mg/mL protein X. Table 4 compares the increase in aggregate content and scattering intensity on heating 2, 5, 20 and 50 mg/mL protein X samples for 1, 2 and 3 hours. On heating for 3 hours the percent aggregates increased to 10 and 15% respectively, for 2 and 5 mg/mL protein X. A significant change in scattering intensity was also observed at longer heating times and can be qualitatively compared to the increase in aggregates (measured using SEC). For example, scattering intensity of 2 mg/mL protein X increased by a factor of 1.2 (3.8% aggregates) at 2 hours and a factor of 1.5 (10.2% aggregates) at 3 hours of heating. In dilute protein solutions, lower concentration of small sized aggregates are formed and the presence of more than 4% aggregates can be detected using UV light scattering intensity.

On heating 20 mg/mL protein X sample for 1 hour, 3.3% aggregates were formed (measured by SEC) but a significant increase (from T=0) in scattering intensity was not observed. This is because a small change in scattering intensity is observed for low aggregate contentment and is therefore, difficult to analyze. However, longer heating times increased both the percent aggregates and thereby, increase the total scattering intensity for the samples. Similar change in aggregate content and scattering intensity was measured for 50 mg/mL protein X samples on heating.

6.4. Determination of increase in scattering intensity of protein X samples on aggregation

Approximate calculations were performed to determine the increase in scattering intensity on aggregation, by assuming that only dimers are formed on heating the samples. The following calculations were performed for dilute protein X solutions (similar to β-lg analysis):

2 mg/mL protein X			
T = 0	1.2 (2a) + 98.8a =	101.2a	
T = 1 hr	1.7 (2a) + 98.3a =	101.7a	1.01X
T = 2 hr	3.8 (2a) + 96.2a =	103.8a	1.03X
T = 3 hr	10.2 (2a) + 89.8a =	110.2a	1.09X
5 mg/mL protein X			
T = 0	1.3 (2a) + 98.7a =	101.3a	
T = 1 hr	2.0 (2a) + 98.0a =	102.0a	1.01X
T = 2 hr	9.5 (2a) + 90.5a =	109.5a	1.08X
T = 3 hr	15.3 (2a) + 84.7a =	115.3a	1.14X

The following calculations were performed for concentrated protein X solutions:

20 mg/mL protein X			
T = 0	1.0 (2a) + 99.0a =	101.0a	
T = 1 hr	3.3 (2a) + 96.7a =	103.3a	1.02X
T = 2 hr	5.9 (2a) + 94.1a =	105.9a	1.05X
T = 3 hr	8.1 (2a) + 91.9a =	108.1a	1.07X
50 mg/mL protein X			
T = 0	1.0 (2a) + 99.0a =	101.0a	
T = 1 hr	5.7 (2a) + 94.3a =	105.7a	1.05X
T = 2 hr	10.2 (2a) + 89.8a =	110.2a	1.09X
T = 3 hr	13.4 (2a) + 86.6a =	113.4a	1.12X

The increase in light scattering determined by approximate calculations (shown above) are qualitatively comparable to the experimentally measured increase in light scattering (shown in table 4). The values for dilute solution calculations are closer to the measured values. However, at higher concentrations aggregates of larger size will be formed that contribute to the scattering intensity. Therefore, the change in scattering intensity calculations should include formation of higher order aggregates (other than dimers) to get better estimate of aggregate content.

These studies demonstrate that UV light scattering can be used for detecting an increase in percent aggregates for both dilute and medium protein concentrations. The greatest advantage of this technique is reduced preparation and analysis times, by eliminating sample dilutions, column equilibration, need for different mobile phases that is typical for SEC analysis. UV light scattering can be used to detect both soluble and insoluble aggregates. Furthermore, it also has the potential of detecting self-association (demonstrated previously in chapter 4). UV light scattering can be

used as a high throughput technique with 96 well plate readers and can measure sample concentration along with detecting self-association and aggregation of proteins.

Information regarding the properties and distribution of protein aggregates requires further characterization using techniques like SE-HPLC or AUC.

7. SUMMARY AND CONCLUSIONS

Similar to SEC (the industry standard), UV light scattering can be used to track aggregation in proteins with an added advantage of being able to analyze both soluble and insoluble aggregates. Additionally, one of the major advantage of this technique is that the protein samples can be analyzed at the same concentrations at which they are formulated i.e. it eliminates the need to dilute the samples before analysis providing a more representative analysis of aggregation. The study shows that UV light scattering can be used as a rapid and economic tool for detecting aggregates to screen lead candidates.

8. REFERENCES

1. Shire, S. J.; Shahrokh, Z.; Liu, J. Challenges in the development of high protein concentration formulations. *J. Pharm. Sci.* **2004**, *93*, 1390-1402.

2. Cleland, J. L.; Powell, M. F.; Shire, S. J. The development of stable protein formulations: A close look at protein aggregation, deamidation, and oxidation. *Crit. Rev. Ther. Drug Carrier Syst.* **1993**, *10*, 307-377.

3. Roberts, C. J. Protein aggregation and its impact on product quality. *Curr. Opin. Biotechnol.* **2014**, *30*, 211-217.

4. Jiskoot, W.; Randolph, T. W.; Volkin, D. B.; Middaugh, C. R.; Schöneich, C.; Winter, G.; Friess, W.; Crommelin, D. J. A.; Carpenter, J. F. Protein instability and immunogenicity: Roadblocks to clinical application of injectable protein delivery systems for sustained release. *J. Pharm. Sci.* **2012**, *101*, 946-954.

5. Narhi, L. O.; Schmit, J.; Bechtold-Peters, K.; Sharma, D. Classification of protein aggregates. *J. Pharm. Sci.* **2012**, *101*, 493-498.

6. Amin, S.; Barnett, G. V.; Pathak, J. A.; Roberts, C. J.; Sarangapani, P. S. Protein aggregation, particle formation, characterization & rheology. *Curr. Opin. Colloid Interface Sci.* **2014**, *19*, 438-449.

7. Bajaj, H.; Sharma, V. K.; Kalonia, D. S. A high-throughput method for detection of protein self-association and second virial coefficient using size-exclusion chromatography through simultaneous measurement of concentration and scattered light intensity. *Pharm. Res.* **2007**, *24*, 2071-2083.

8. Eisenberg, H.; Tomkins, G. M. Molecular weight of the subunits, oligomeric and associated forms of bovine liver glutamate dehydrogenase. *J. Mol. Biol.* **1968**, *31*, 37-49.

9. Roberts, C. J. Therapeutic protein aggregation: Mechanisms, design, and control. *Trends Biotechnol.* **2014**, *32*, 372-380.

10. Wu, S.; Ding, Y.; Zhang, G. Mechanic Insight into Aggregation of Lysozyme by Ultrasensitive Differential Scanning Calorimetry and Sedimentation Velocity. *J Phys Chem B* **2015**, *119*, 15789-15795.

11. Kumar, V.; Dixit, N.; Zhou, L.; Fraunhofer, W. Impact of short range hydrophobic interactions and long range electrostatic forces on the aggregation kinetics of a monoclonal

antibody and a dual-variable domain immunoglobulin at low and high concentrations. *Int. J. Pharm.* **2011**, *421*, 82-93.

12. Chari, R.; Singh, S. N.; Yadav, S.; Brems, D. N.; Kalonia, D. S. Determination of the dipole moments of RNAse SA wild type and a basic mutant. *Proteins Struct. Funct. Bioinformatics* **2012**, *80*, 1041-1052.

13. Borzova, V. A.; Markossian, K. A.; Chebotareva, N. A.; Kleymenov, S. Y.; Poliansky, N. B.; Muranov, K. O.; Stein-Margolina, V. A.; Shubin, V. V.; Markov, D. I.; Kurganov, B. I. Kinetics of thermal denaturation andaggregation of bovine serum albumin. *PLoS ONE* **2016**, *11*.

14. Blake, S.; Amin, S.; Qi, W.; Majumda, M.; Lewis, E. N. Colloidal stability & conformational changes in ß-lactoglobulin: Unfolding unfolding to self-assembly. *Int. J. Mol. Sci.* **2015**, *16*, 17719-17733.

15. Aymard, P.; Gimel, J. C.; Nicolai, T.; Durand, D. Experimental evidence for a two-step process in the aggregation of ß-lactoglobulin at pH 7. *J. Chim. Phys. Phys. -Chim. Biol.* **1996**, *93*, 987-997.

16. Pace, C. N.; Vajdos, F.; Fee, L.; Grimsley, G.; Gray, T. How to measure and predict the molar absorption coefficient of a protein. *Protein Science* **1995**, *4*, 2411-2423.

9. Tables

Table 1. Properties of the model proteins used for the studies

Protein	Abbreviation	$\varepsilon^{1mg/mL}$ (mL/mg*cm) at 280 nm	MW (kDa)
β-lactoglobulin (A&B mix)	β-lg	0.960*	18.4*
Bovine serum albumin	BSA	0.661*	67.0*
Protein X	--	1.500	149.0

*Pace et al. 1995.[16]

Table 2. Comparison of the change in amount of soluble aggregates and light scattering intensities before (T = 0) and after heating 20 mg/mL β-lg at 65 ºC for 3, 5 and 6 hours.

I.

Heating time	Percent Aggregate	Percent Dimer	LS Intensity	**Increase in LS from T=0***
T = 0		100	170,199	
T = 3 hr	13	87	412,910	**2.4X**
T = 5 hr	33	67	857,569	**5.0X**
T = 6 hr	40	60	1,026,606	**6.0X**

II.

Heating time	Approximate calculation of scattering contribution+			**Increase in LS from T=0***
	Aggregates	Dimers	Total	
T = 0		100a	100a	
T = 3 hr	13 * 8a	87a	191a	**1.9X**
T = 5 hr	33 * 8a	67a	331a	**3.3X**
T = 6 hr	40 * 8a	60a	380a	**3.8X**

* The change in scattering intensity is the ratio of scattering intensity of β-lg samples after heating for 3, 5 and 6 hours to scattering intensity before heating (T = 0).

+ Approximate calculations of scattering intensity contribution of each sample was performed using the following assumptions:
  1) Molecular weight is the only factor effecting the total scattering intensity of the sample.
  2) 'a' is the average molecular weight of β-lg species before heating (T =0).
  3) The molecular weight of aggregates is 8a. The approximation was based on the elution time of the aggregate peak.
  4) Percent aggregates and dimers measured by SEC were used as the concentration of those species in the samples.

Table 3. Comparison of the change in amount of soluble aggregates and light scattering intensities before (T = 0) and after heating 50 mg/mL β-lg at 65 ºC for 1, 2 and 3 hours.

I.

Heating time	Percent Aggregate	Percent Dimer	LS Intensity	**Increase in LS from T=0***
T = 0		100	313150	
T = 1 hr	2	98	350126	**1.1X**
T = 2 hr	26	74	956758	**3.1X**
T = 3 hr	45	55	1413876	**4.5X**

II.

Heating time	Approximate calculation of scattering contribution+			**Increase in LS from T=0***
	Aggregates	Dimers	Total	
T = 0		100a	100a	
T = 1 hr	2 * 8a	98a	112a	**1.1X**
T = 2 hr	26 * 8a	74a	283a	**2.8X**
T = 3 hr	45 * 8a	55a	412a	**4.1X**

* The change in scattering intensity is the ratio of scattering intensity of β-lg samples after heating for 1, 2 and 3 hours to scattering intensity before heating (T = 0).
+ Same as Table 2.

Table 4. Comparing the increase in percent aggregates (measured by SEC) and scattering intensity (measured at 350 nm) on heating 2, 5, 20 and 50 mg/mL Protein X for 1, 2 and 3 hours.

Protein Concentration (mg/mL)	Percent Aggregates[+]			Change in scattering intensity*		
	T= 1 hr	T= 2 hrs	T= 3 hrs	T= 1 hr	T= 2 hrs	T= 3 hrs
2	1.7	3.8	10.2	1.0X	1.2X	1.5X
5	1.9	9.5	15.3	1.0X	1.3X	1.6X
20	3.3	5.9	8.1	1.0X	1.3X	1.6X
50	5.7	10.2	13.4	1.1X	1.5X	2.1X

+ 2 and 5 mg/mL protein X samples contained 1.3% aggregates at T = 0 and were heated at 65 ºC. 20 and 50 mg/mL protein X samples contained 1% aggregates at T = 0 and were heated at 63 ºC.

* The change in scattering intensity is the ratio of scattering intensity of Protein X samples after heating for 1, 2 and 3 hours to scattering intensity before heating (T = 0).

10. Figures

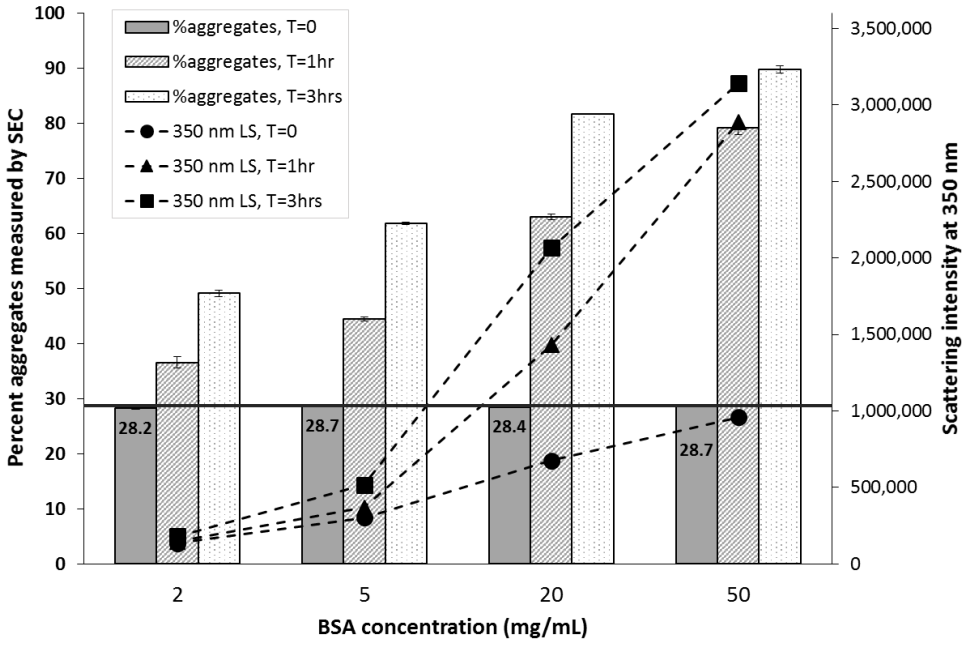

Figure 1. Percent aggregates (primary y-axis) and scattering intensity (secondary y-axis) as function of BSA concentration. The bar graph represents percent soluble aggregates measured using SE-HPLC. Mobile phase: Phosphate buffer pH 7.0 and ionic strength 200 mM. The scattering intensities measured before heating (T = 0) are represented by circles and after heating at 58 ºC for 1 and 3 hours by triangles and squares, respectively. The lines connecting the data points are only to guide the eye of the reader and are not a result of fitting a model to the data. The solid black line represents the presence of 28.5% aggregates before heating the samples (T = 0).

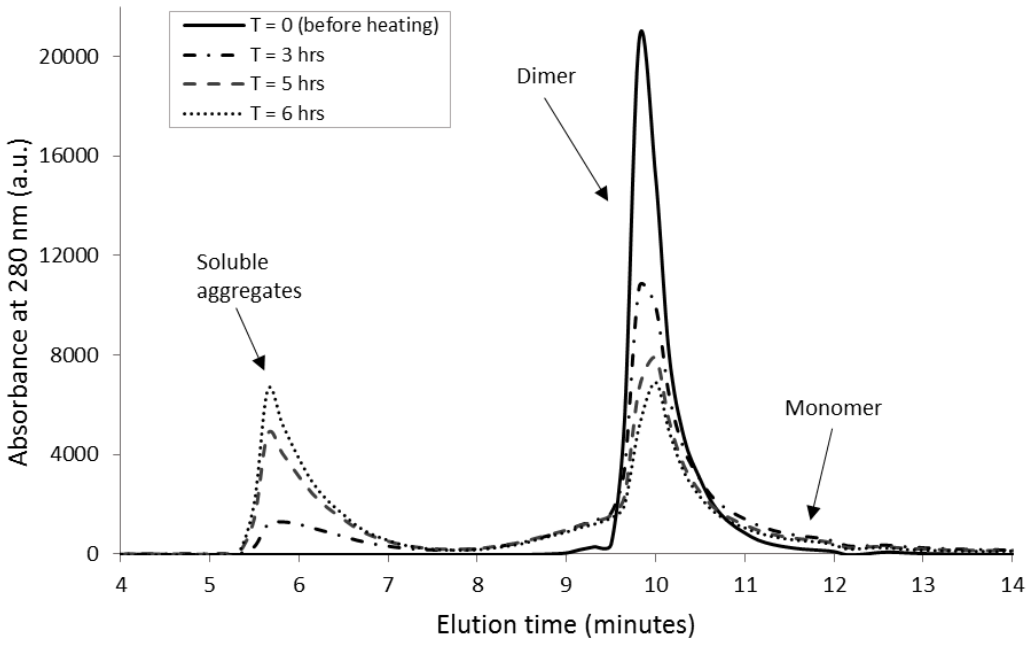

Figure 2. UV chromatograms (280 nm) for β-lg solutions before (T = 0) and after heating 20 mg/mL sample at 65 ºC for 3, 5 and 6 hours. All the samples were diluted to 2 mg/mL concentration before obtaining the chromatogram. Mobile phase: Phosphate buffer pH 7.0 and ionic strength 200 mM.

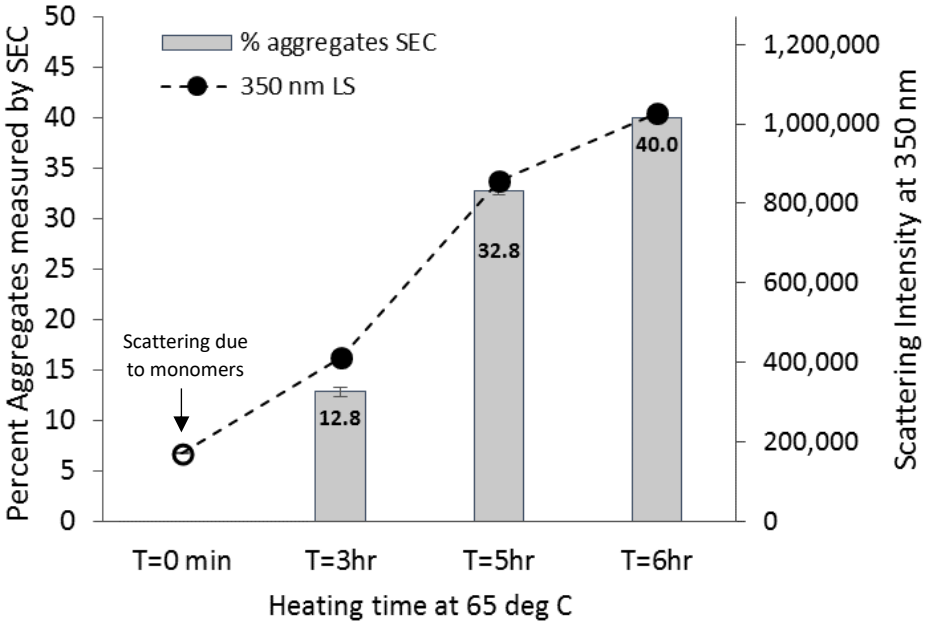

Figure 3. Percent aggregates measured by SEC (primary y-axis) and light scattering intensity measured at 350 nm (secondary y-axis) for β-lg solutions before (T = 0) and after heating 20 mg/mL sample at 65 ºC for 3, 5 and 6 hours. The bar graph represents percent soluble aggregates calculated using SE-HPLC for 20 mg/mL β-lg diluted to 2 mg/mL. Mobile phase: Phosphate buffer pH 7.0 and ionic strength 200 mM. The circles represent static light scattering intensities of 20 mg/mL β-lg measured without any further dilution. The lines connecting the data points are only to guide the eye of the reader and are not a result of fitting a model to the data.

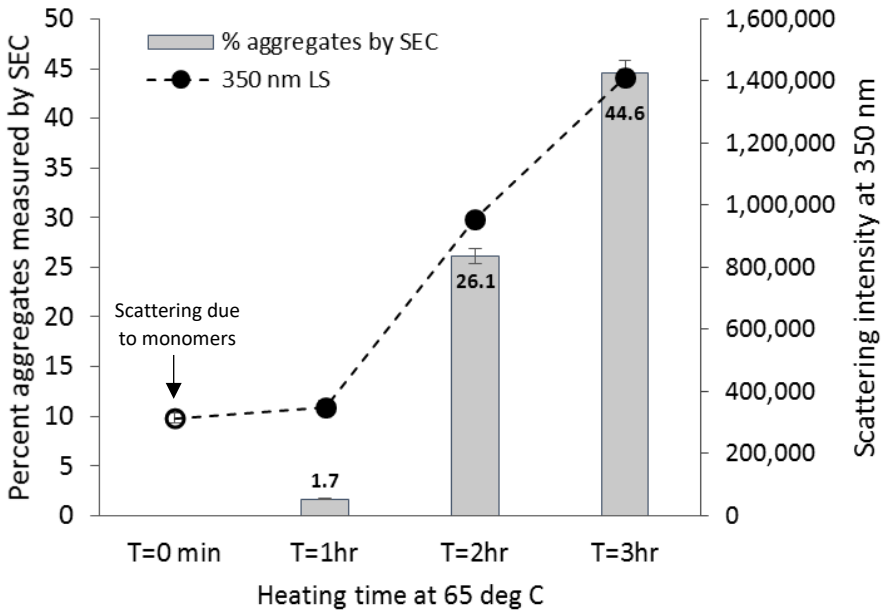

Figure 4. Percent aggregates measured by SEC (primary y-axis) and light scattering intensity measured at 350 nm (secondary y-axis) for β-lg solutions before (T = 0) and after heating 50 mg/mL sample at 65 ºC for 1, 2 and 3 hours. The bar graph represents percent soluble aggregates calculated using SE-HPLC for 50 mg/mL β-lg diluted to 2 mg/mL. Mobile phase: Phosphate buffer pH 7.0 and ionic strength 200 mM. The circles represent static light scattering intensities of 50 mg/mL β-lg measured without any further dilution. The lines connecting the data points are only to guide the eye of the reader and are not a result of fitting a model to the data.

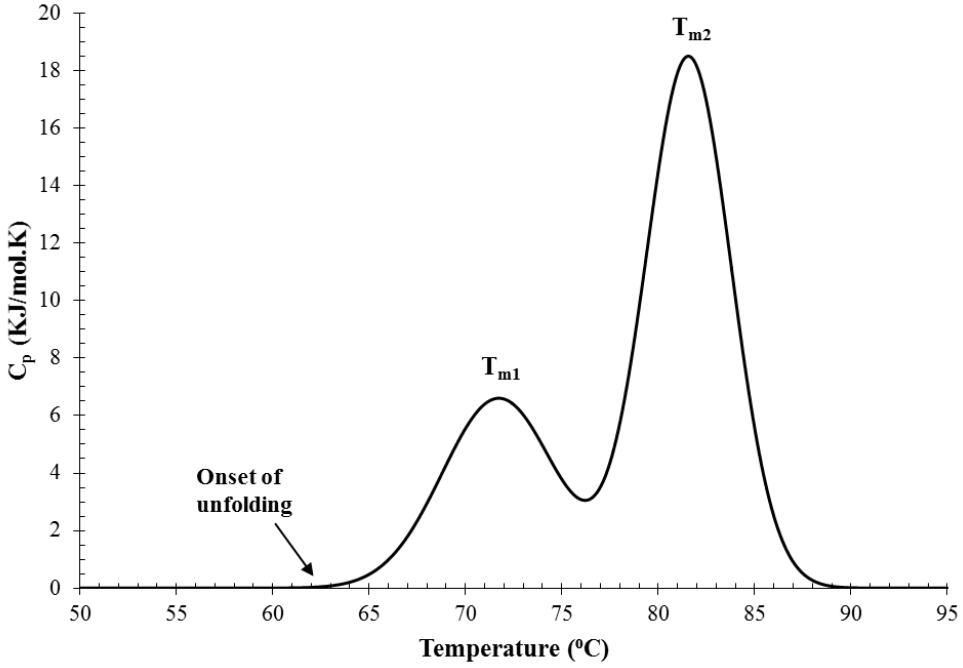

Figure 5. Thermal unfolding scan obtained by differential scanning calorimetry (DSC) for 1 mg/mL protein X in 15 mM phosphate buffer at pH 7.

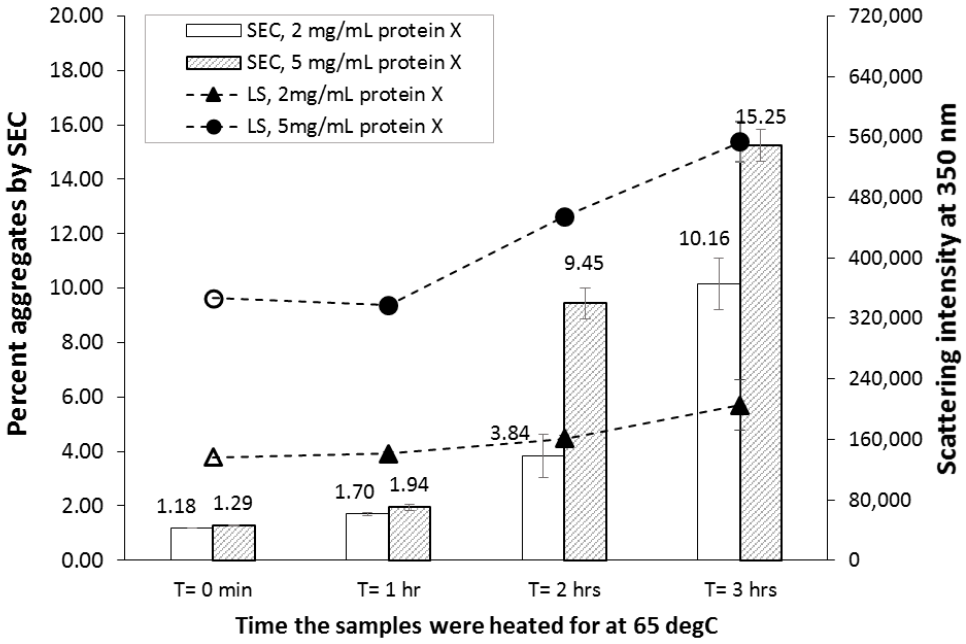

Figure 6. Percent aggregates measured by SEC (primary y-axis) and light scattering intensity measured at 350 nm (secondary y-axis) for protein X solutions before (T = 0) and after heating 2 and 5 mg/mL samples at 65 ºC for 0, 1, 2 and 3 hours. The bar graphs represent percent soluble aggregates calculated using SE-HPLC. The open symbols represent initial scatter intensity and closed symbols represent scattering intensities of samples after heating. The lines connecting the data points are only to guide the eye of the reader and are not a result of fitting a model to the data.

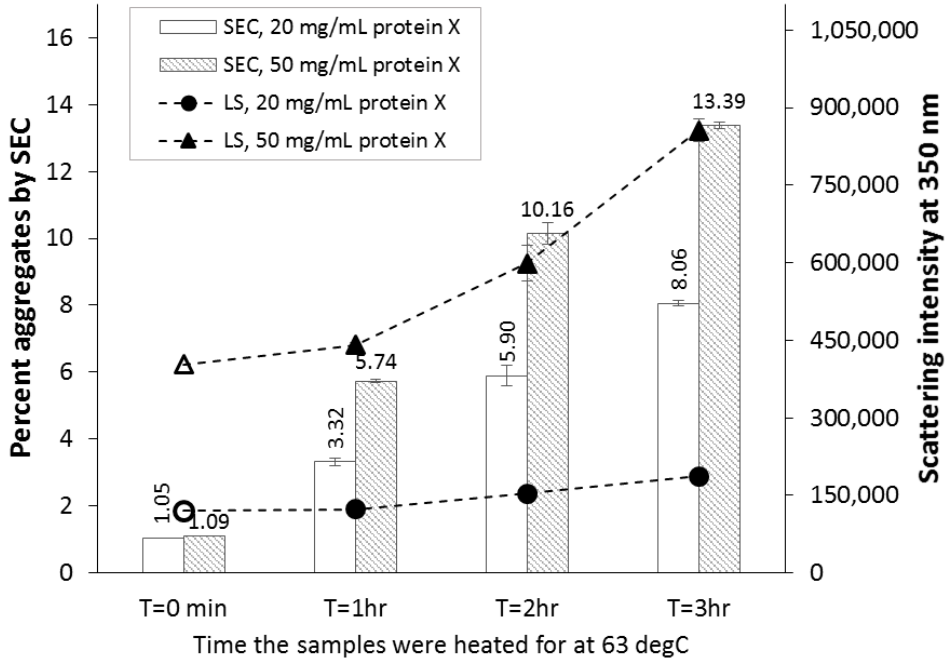

Figure 7. Percent aggregates measured by SEC (primary y-axis) and light scattering intensity measured at 350 nm (secondary y-axis) for protein X solutions before (T = 0) and after heating 20 and 50 mg/mL samples at 63 ºC for 0, 1, 2 and 3 hours. The bar graphs represent percent soluble aggregates calculated using SE-HPLC. The open symbols represent initial scatter intensity and closed symbols represent scattering intensities of samples after heating. The lines connecting the data points are only to guide the eye of the reader and are not a result of fitting a model to the data.

Chapter 6

Summary

Reversible (self-association) and irreversible aggregation are two of the major degradation pathways for proteins in solution. Reversible aggregates can increase solution viscosity, decrease bioavailability and/or lead to the formation of irreversible aggregates. Furthermore, irreversible aggregates can cause immunogenic reactions and decrease drug potency. Therefore, aggregation (both reversible and irreversible) negatively affects manufacturing, delivery and product quality, making it critical to analyze protein aggregation behavior in an early development stage. Static light scattering is one of the most successful techniques to characterize different properties of proteins in solution. A review of the applications of static light scattering with a focus on characterizing molecular weight, protein-protein interactions, self-association and aggregation of proteins was discussed in **Chapter 2**. The basic instrumentation and limitations associated with present light scattering techniques were summarized. Based on the literature review, discussion about the scope of static light scattering as a tool to analyze proteins at a wide range of concentrations and solution conditions was made.

Static light scattering intensity has an inverse fourth power dependence on the wavelength of incident light. Thereby, using shorter wavelengths in UV range can increase the sensitivity of the technique. The current static light scattering techniques use light sources with wavelengths greater than 600 nm to avoid interference from other optical phenomena such as chromophoric absorption by protein residues. A systematic investigation of the effect of absorption on 90º Rayleigh scattering and turbidity measurements was performed in **Chapter 3**. The results showed that turbidity of macromolecules was unaffected by the presence of absorbing molecules. However, 90º Rayleigh scattering intensities decreased at wavelengths where absorption was significant. Thereby, the scattering intensity decrease was observed due to

reabsorption of scattered light by the protein chromophores and depends on molar absorptivity, molecular weight and concentration of proteins.

The studies and results reported in **Chapter 4** showed the ability to develop ultraviolet light scattering as a high-throughput technique to detect reversible self-association in protein formulations. Solution conditions (pH and ionic strength) and protein concentration based self-association was studied using β-lactoglobulin A and glutamate dehydrogenase (GDH), respectively as model proteins. The results show that when a single species (monomer or dimer) was present, the scattering intensity was directly proportional to protein concentration, as seen in the case of β-lactoglobulin A and the slope was related to the molecular weight of the species. However, when more than one type of species were present (i.e. a mix of monomer, dimer or other oligomers), a non-linear increase in scattering intensity was observed as seen in the case of GDH. The studies demonstrate that UV light scattering can be used as a fast and rapid tool for detecting self-association in proteins. Additionally, it can be used to screen different solution pH and ionic strengths to optimize formulations at an early development stage.

The studies to investigate the application of ultraviolet static light scattering to detect change in aggregate content for protein formulations in the concentration range of 2 – 50 mg/mL was reported in **Chapter 5.** Bovine serum albumin, β-lactoglobulin and a monoclonal antibody were used for this purpose. The results demonstrate that UV light scattering can be used to detect aggregation in proteins with an advantage of being able to analyze both soluble and insoluble aggregates. Additionally, one of the major advantage of this technique is that the protein samples can be analyzed at the same concentrations at which they are formulated i.e. it eliminates the need to dilute the samples before analysis providing a more representative

analysis of aggregation. This work plays a critical role in expanding the application of static light scattering to the ultraviolet range and systematically investigating its use for detecting reversible and irreversible aggregation in protein solutions.

SYMBOLS

A, Absorbance of sample

a_{abs}, Absorption coefficient

K_a, Association constant

N_A, Avogadro's number

B_2, Thermodynamic second virial coefficient

c, Concentration of the scattering molecule (mg/mL)

w, Concentration of the scattering molecule (g/mL)

H, Constant related to the optical constant K

r, Distance between the scattering molecule and the detector (cm)

I, Intensity of transmitted light

I_0, Intensity of incident light

M_w, weight-average Molecular weight of the scattering molecule (Da)

i_s, Time-average scattering intensity

γ, Thermodynamic activity coefficient

τ, Turbidity of solution

K, Optical constant

l, Path length (cm)

R_g, Radius of gyration of the scattering particles

R_θ, (excess) Rayleigh scattering ratio

n, Refractive index of solution

n_0, Refractive index of solvent

dn/dc, Refractive index gradient for the solvent/scattering molecule pair

θ, Scattering angle

λ_0, Wavelength of incident light in vacuum